

TECHNICAL REPORT NO. 95

Subwatershed Monitoring in the McKenzie Brook Watershed in Vermont



October 2019

Final Report

Prepared by:

Blaine Hastings
Angie R. Allen
Sean Regaldo
Vermont Department of Environmental Conservation,
Watershed Management Division

For:

The Lake Champlain Basin Program and
New England Interstate Water Pollution Control Commission

This report was funded and prepared under the authority of the Lake Champlain Special Designation Act of 1990, P.L. 101-596 and subsequent reauthorization in 2002 as the Daniel Patrick Moynihan Lake Champlain Basin Program Act, H. R. 1070, through the US EPA and the Great Lakes Fishery Commission. Publication of this report does not signify that the contents necessarily reflect the views of the states of New York and Vermont, the Lake Champlain Basin Program, the Great Lakes Fishery Commission, or the US EPA.

The Lake Champlain Basin Program has funded more than 90 technical reports and research studies since 1991. For complete list of LCBP Reports please visit:
<http://www.lcbp.org/media-center/publications-library/publication-database/>

Subwatershed Monitoring in the McKenzie Brook Watershed in Vermont

October 2019

Final Report

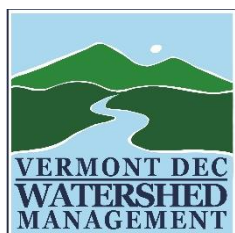


Prepared by:

Blaine Hastings and **Angie R. Allen**, with geospatial processing assistance from **Sean Regalado**

Vermont Department of Environmental Conservation,

Watershed Management Division



Executive Summary

A phosphorus loading study was conducted for the Vermont portion of the agriculturally dominated Mckenzie Brook watershed, which drains several small subwatersheds directly to the southern portion of Lake Champlain. Water quality (7 sites), streamflow (2 gages), and precipitation (12 gages) monitoring was conducted from April – November in both calendar years 2017 and 2018. 342 total and dissolved phosphorus samples were collected in 2017, which was characterized by above normal spring-summer rainfall and normal to below normal monthly totals that fall, with a significant 2.59 inch event in early July. 281 total and dissolved phosphorus samples were collected in 2018, which was much drier with above normal rainfall in April and November but well below normal for most of the intervening months and many periods of zero flow. A watershed model based on the curve number approach was developed that includes soil moisture accounting routines, which was calibrated and validated to estimate daily mean streamflow at ungaged sampling sites. Poor and inconsistent concentration-discharge correlations necessitated the use of the Beale Ratio Estimator to estimate flow-weighted daily mean concentrations and total April - November loads for year at each site. In general, the sampled phosphorus concentrations were high, with some extremely high concentrations even at low flows. This study provided useful insight into the hydrologic and geochemical dynamics of this region, and results serve as a point of reference for reducing phosphorus concentrations and loads through implementation of agricultural best management practices moving forward.

Contents

Executive Summary	2
Introduction	3
Watershed Description	3
Methods	5
Streamflow gaging	5
Rating curve development	7
Precipitation monitoring	10
Water quality sampling	12
Laboratory QA/QC	12
Rainfall-runoff model for ungaged sampling sites	13
Calculation of nutrient loads	17
Results	20
Precipitation	20
Observed Streamflow	21
Modeled Streamflow	24
Water Chemistry	27
Loading Calculations	34
Sources of uncertainty	38
References	40

Introduction

The Vermont portion of the HUC-12 “McKenzie Brook Watershed” is a composite of several subwatersheds in western Addison County that drain directly into Lake Champlain’s “South Lake”. This is one of the most intensive agricultural areas in the State of Vermont. It is part of what is known as Lake Segment A, which requires a 60% reduction in phosphorus loading from agricultural sources to meet State and Federal water quality targets. Recently, the McKenzie Brook Watershed has been targeted by the Natural Resource Conservation Service (NRCS) and its partners for accelerated implementation of agricultural best management practices (BMPs) over the next 5 years. During this timeframe, NRCS technical and financial assistance as well as resources provided by partners will be directed to this watershed.

At the behest of the Lake Champlain Basin Program and NRCS, the Vermont Department of Environmental Conservation (DEC) Monitoring, Assessment, and Planning Program initiated the McKenzie Brook hydrologic and water quality monitoring study to complement on-going and expanding efforts to implement targeted BMP installations on watershed farms. These data were used to document existing conditions in calendar years 2017 and 2018 with respect to streamflows and loading of nutrients. A point of reference using observations specific to these waterbodies is especially valuable as the size, geology, stream types and relative land cover/land use within this study area differ considerably from other monitoring and loading studies conducted in the Lake Champlain Basin (Medalie, 2016; Vaughan, 2019). Insights into the nature of the hydrology and nutrient dynamics for this portion of the basin will be important to consider when conducting further monitoring and BMP implementations aimed at reducing nutrient loading to streams.

Watershed Description

The McKenzie Brook study area consists of approximately 21,000 acres of small subwatersheds draining directly to the southern portion of Lake Champlain (Figure 1). It is a lower elevation rolling landscape dominated by agricultural land-use and cropland at about 16,350 acres (USDA-NRCS, 2016). 1981-2010 climate normals for the area include average annual precipitation of 35.4 inches, ranging from 1.9 inches in February to around 3.5 inches in July. Average annual temperature was 56.8°F, with monthly averages ranging from 20°F in January to 71°F in August (PRISM, 2019). Seven subwatersheds were selected as water quality monitoring sites for which nutrient loads were estimated (Table 1).

Table 1: water quality sampling sites

Site Location	Latitude (NAD83)	Longitude (NAD83)	Drainage area (acres)
Hospital Creek at Country Club Rd. (Addison, VT)	44.05346° N	73.38994° W	688
Wards Creek at Jersey St. (Addison, VT)	44.0384° N	73.37032° W	1,194
West Branch Dead Creek at streamflow gage at Middle Rd. (Bridport, VT)	43.97829° N	73.36541° W	2,683
Braisted Brook at Lake Street (Bridport, VT)	43.97782° N	73.39721° W	1,501
Stony Creek at mouth (Shoreham, VT)	43.8998° N	73.3723° W	922
North Fork East Creek at streamflow gage below VT RT-73 (Orwell, VT)	43.82705° N	73.32294° W	6,995
North Fork East Creek at Old Foundry Rd (Orwell, VT)	43.80959° N	73.33159° W	7,865

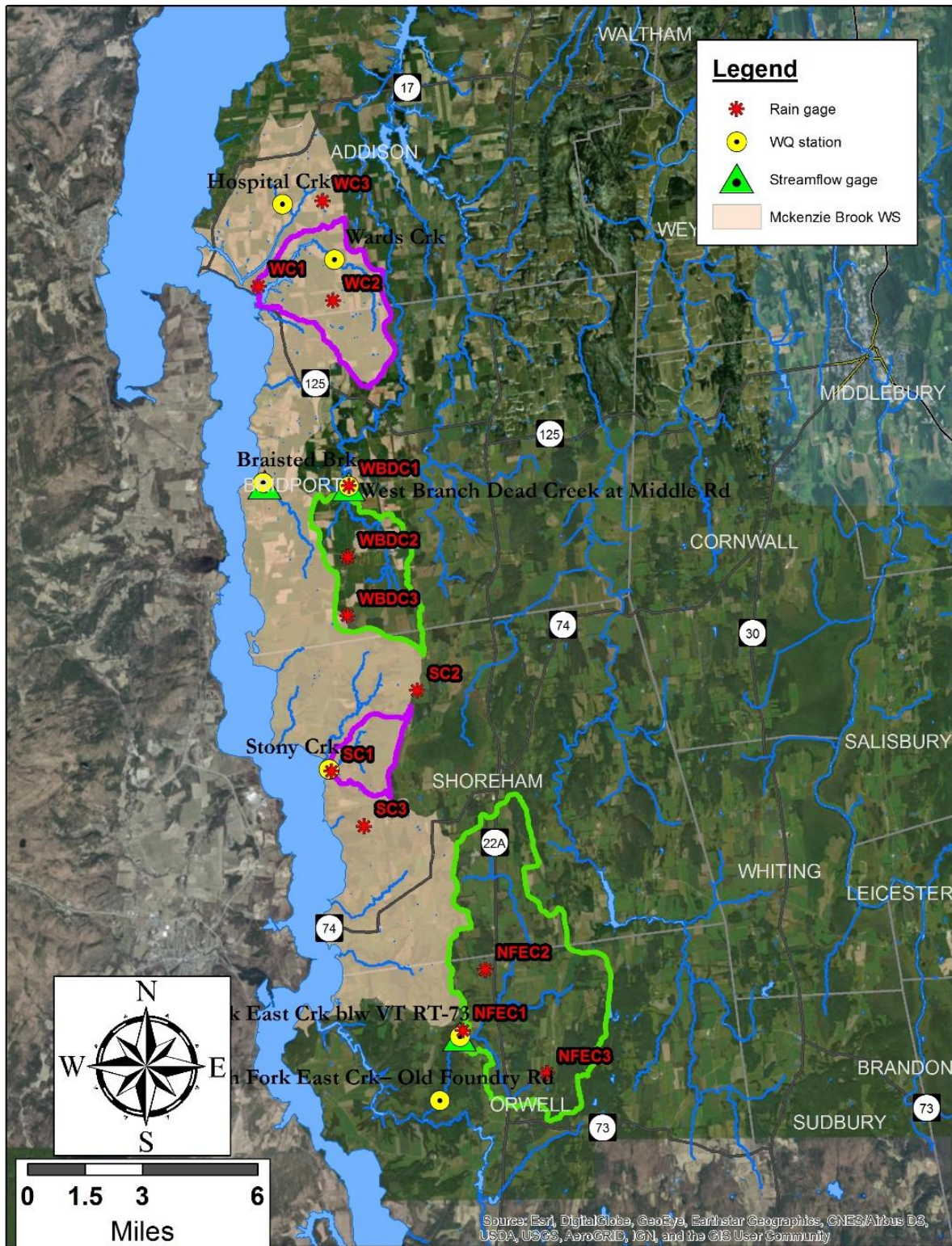


Figure 1: Map of the McKenzie Brook study area with 7 water quality sampling sites, 12 rainfall gaging stations, and 2 streamflow gaging stations in adjacent watersheds.

Methods

Streamflow gaging

Continuous-recording streamflow gages were constructed and operated at two locations: West Branch Dead Creek at Middle Rd. in Bridport, VT (“WBDC1”) and North Fork East Creek (“NFEC1”) below VT Route 73 in Orwell, VT (Figure 1). These locations were selected as the only suitable locations for operating standard stage-discharge streamflow gaging stations. Siting considered the hydraulic characteristics, but their relatively larger drainage areas also meant they would have streamflow for longer portions of the year which allowed for extrapolation of flows to other watersheds. This would have been more difficult were smaller more intermittent streams used as index streamflow monitoring stations.

- **West Branch Dead Creek at Middle Rd., Bridport, VT (Figure 2):** This stream is outside of the target watershed; however, it is adjacent and much of the drainage area is within the north-south extent of the study area. A new corrugated metal culvert encased in concrete walls carries the West Branch Dead Creek below Middle Rd. There was little head loss through the culvert, and the culvert itself does not provide a constriction to streamflows under normal to low-flow conditions. A pool is formed by an earthen constriction downstream of Middle Road, providing hydraulic control for the pool extending upstream several meters above the culvert. This is a less sensitive site in terms of water level rise in response to a given increase in streamflow, but was stable, accessible, and was estimated to maintain some flow much of the year.
- **North Fork East Creek below VT-73, Orwell, VT (Figure 3):** This streamflow gage is also in an adjacent subwatershed and was installed approximately 0.35 miles below the highway at a bedrock outcrop which forms a pool that provides stable section control. The reach is straight upstream and downstream of the site and was observed to maintain flow during very low-flow conditions of the initial reconnaissance visit.

A temporary stream gage was deployed at the Lake Street culvert on Braisted Brook for additional runoff model validation data. However, it was not installed until July 2017 and the mounting hardware was lost during the winter/spring of 2018. It was decided not to replace the equipment and a valid rating curve was never finalized. An unsurveyed depth-only water level logger and open-air barometer were also deployed during portions of both years near the mouth of Stony Creek to support qualitative runoff model validation against timing of hydrograph rises. Subsequent analysis of LiDAR elevation data revealed the influence of lake level inundation that confounded the utility of this dataset. Valid observations of free-flowing stream rises were thus sparser and ultimately of little value for model evaluation.

Gaging procedures generally followed those of Rantz et al. (1982), Turnipseed and Sauer (2010) and U.S. EPA (2014). Each station was equipped with submersible logging pressure transducers encased in PVC stilling wells, with an additional pressure transducer mounted above water level to provide barometric correction to calculate stage. Transducers had a depth accuracy of within ± 0.015 ft. and logged measurements every 15-minutes. Differential water level accuracy was lab-tested and verified via “bucket tests” preceding each monitoring season. A secondary water level logger was deployed approximately 40 meters upstream at the NFEC gage to calculate water surface slope during high flow events. Three elevation benchmarks were established at each site and regularly surveyed to detect any physical shifts in the gage itself and serve as the datum for stream stage values. These datums were also used to record reference water levels at each visit to correct the stage record for any sensor drift and equipment shifts. Time-interpolated corrections to the stage record were applied where the difference between logged water level and measured reference water level was greater than 0.015 ft.



Figure 2: West Branch Dead Creek at Middle Rd (Bridport, VT) streamflow gaging site.

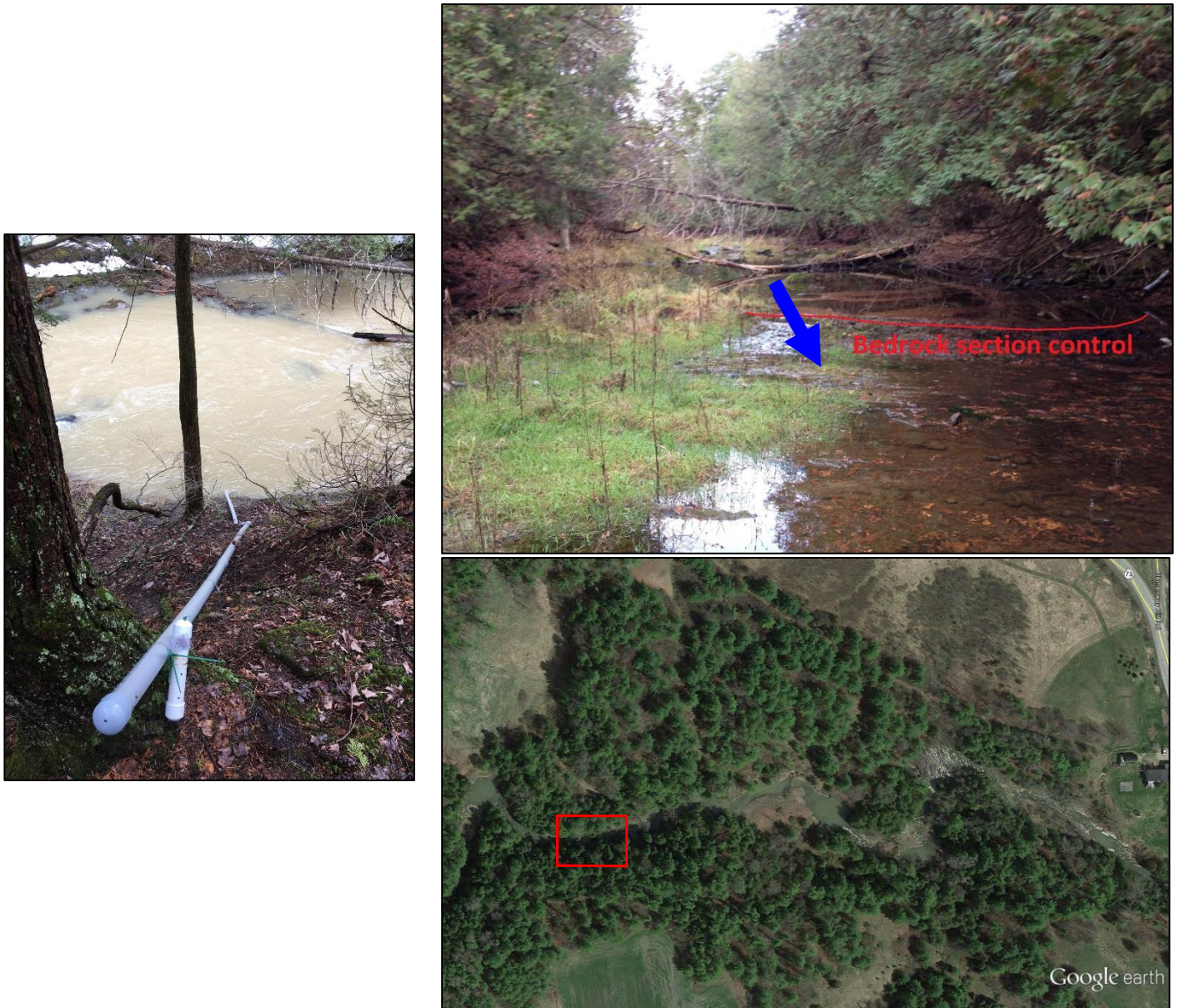


Figure 3: North Fork East Creek at flow gage below VT RT-73 (Orwell, VT) streamflow gaging site.

Rating curve development

Discharge measurements were collected periodically over a range of flows (Tables 2a and 2b) to develop a stage-discharge relationship and estimate streamflow from corrected 15-minute stage data. The stage-discharge rating takes the form of a power function as in equation 2,

$$Q = C(h - GHZ)^n \quad \text{Eq. 2}$$

where Q is discharge, h is reference water level, GHZ is gage height of zero flow, and C and n are determined via regression of $(h - GHZ)$ against discharge. For this study C and n were optimized to minimize the sum of squared errors in the power regression model. Subtracting GHZ from the corrected reference water level expresses water level in terms of “head” above the downstream control. GHZ for each site was calculated indirectly using discharge measurements and the Johnson method (Rantz, 1982), and verified via elevation survey where possible. This is a useful approach as impacts caused by scour, icing, vegetative growth, leaf litter, etc., are effectively shifts in the GHZ and will permanently or temporarily change the stage-discharge relationship. For example, growing vegetation gradually

increases the effective *GHZ* such that the rating curve falsely estimates flows to be higher than they are. The *GHZ* aids in applying corrections to derive valid estimated discharges.

Table 2a: Measured discharges at WBDC

Date	WBDC Measured Discharge (cfs)	Date	WBDC Measured Discharge (cfs)
3/29/2017	20.06	9/21/2017	0.11
4/5/2017	29.76	4/2/2018	2.2
5/4/2017	1.42	5/1/2018	9.29
5/26/2017	2.8	5/23/2018	0.08
6/2/2017	3.14	6/12/2018	0
6/26/2017	1.64	8/8/2018	0.01
7/26/2017	0.19	10/3/2018	1.14
9/7/2017	7.19	11/7/2018	10.09

Table 2b: Measured discharges at NFEC.

*estimated peak flow using slope-area method

Date	NFEC Measured Discharge (cfs)	Date	NFEC Measured Discharge (cfs)
3/31/2017	21.75	10/20/2017	0.12
4/5/2017	74.06	3/28/2018	26.3
5/4/2017	8.90	5/1/2018	31.26
5/26/2017	4.40	6/12/2018	0.13
6/9/2017	4.57	8/8/2018	0.53
6/26/2017	5.90	9/7/2018	0.01
7/2/2017	473.48*	10/3/2018	0.46
8/28/2017	0.23	11/7/2018	16.47
9/7/2017	12.7		

The stage-discharge rating was complicated and variable for the WBDC1 site. A base rating was established using only measurements conducted with a clean control (Figure 4). By comparing measured discharges against the base rating, it was concluded that the site experienced backwater conditions due to vegetative growth in the control at the outlet of the gage pool. For each discharge measurement taken during backwater influenced conditions, the effective shift in *GHZ* could be calculated according to the discharge-stage relationship in the base rating. When this correction is applied to the reference water level at the time of measurement it provides a stage true to the original *GHZ*, and that can be applied with the base rating to get a valid estimated discharge. The vegetative backwater effects began in early May during the start of the growing season and appeared to influence stage in a variable fashion. There was little apparent influence at flows below 0.25 ft., a gradually increasing influence over time as a function of stage from 0.25 – 0.50 ft., and a more stable increasing influence as a function of only time above 0.50 ft. Periods of shifting effective *GHZ* were identified in the record and the degree of this shift at the end of that period was calculated. A time-interpolated correction was applied to the stage record during this period, adjusted by a factor proportional to the stage magnitude between 0.25 and 0.50 ft., and then normally with time at stages above 0.50 ft. The influence of vegetation and the nature of hydraulic control transitioned at higher flows, so backwater corrections were only applied to ($h - GHZ$) values above 4.0 ft.

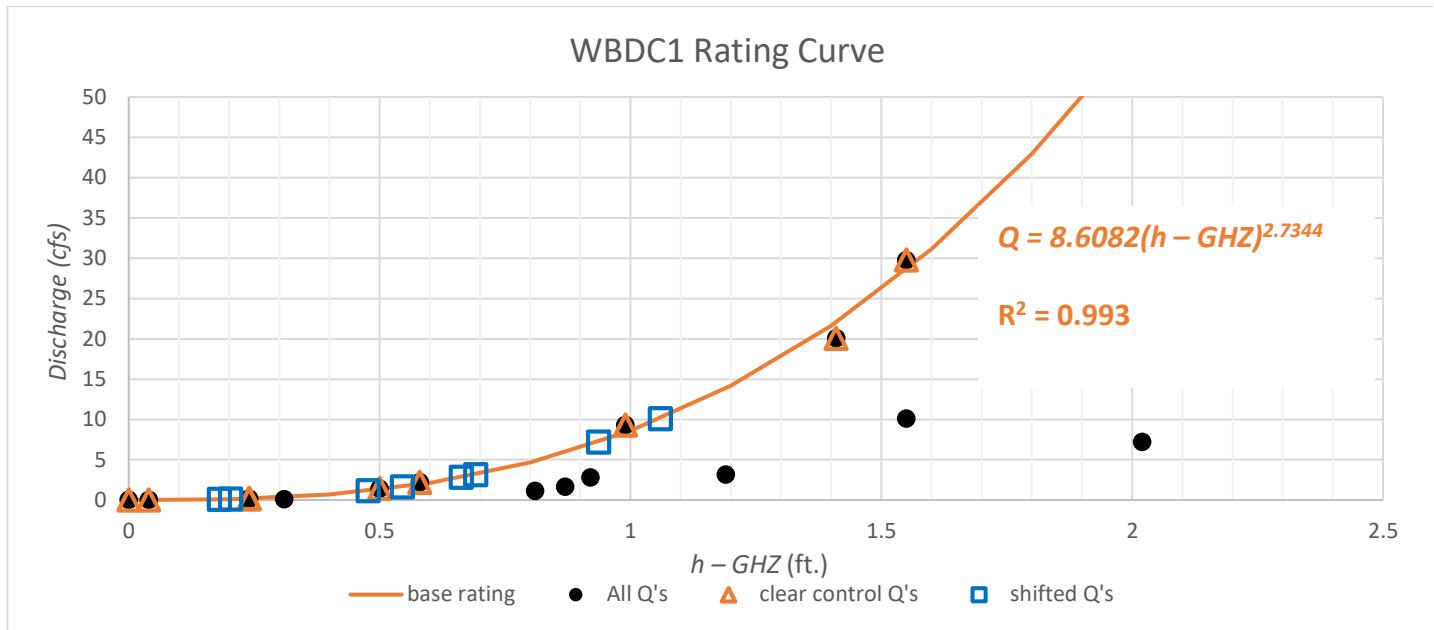


Figure 4: Rating curve and shifts for WBDC1.

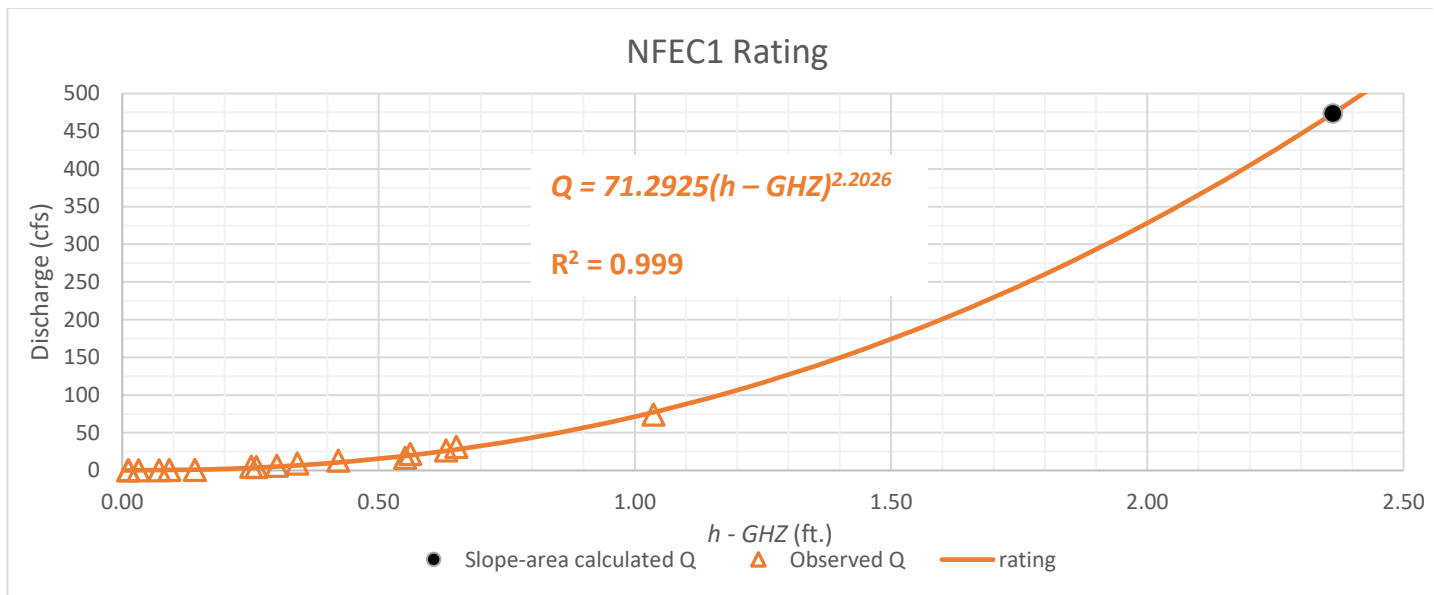


Figure 5: Rating curve for NFEC1.

The stage-discharge relationship for NFEC1 (Figure 5) was much more reliable owing to preferable hydraulic characteristics of the reach and control. This site had an upstream water level logger used to calculate water level slope. Coupled with cross-sectional surveys of the reach this provided channel geometry needed to estimate high flow discharges using the slope-area method (Dalrymple and Benson, 1967). This method is based on the Manning's equation (Eq. 2),

$$Q = \frac{1.486}{n} AR^{\frac{2}{3}} S^{\frac{1}{2}} \quad \text{Eq. 2}$$

where n is Manning's Roughness coefficient, A is cross-sectional area, R is hydraulic radius, and S is the friction slope. A very high flow event occurred in early July 2017 and the slope area method was used to estimate peak streamflow during this event. This data point was included in the rating curve at NFEC1 (Figure 5). WBDC1's stream slope was too

shallow in the reach of the gage and so a secondary logger with this approach was not feasible. Because flows were low for much of the study period, the number of measured high flows was less than ideal for both sites.

At the West Branch Dead Creek site, the water level logger's battery prematurely died resulting in 7 days of data loss. Fortunately, conditions were very dry with zero flows before and after the gap, and data for the missing period were estimated based on local rainfall and North Fork East Creek data. Monitoring periods for each stream gage are included in Table 3.

All 15-minute stage and discharge data underwent thorough QA/QC review and questionable values were addressed where needed. 15-minute time-series data were then summarized into both local calendar day mean daily discharge as well as average UTC daily discharge for use with the hydrologic model.

Table 3: Deployment information for streamflow gages.

Site Location:	West Branch Dead Creek at Middle Rd., Bridport, VT (WBDC1)	North Fork East Creek at flow gage below VT RT-73, Orwell, VT (NFEC1)
Drainage area (acres)	2,683	6,995
2017 monitoring period	3/29/2017 – 12/13/2017	3/31/2017 – 12/13/2017
2018 monitoring period	4/2/2018 – 6/25/2018; 7/2/2018 – 11/29/2018	3/28/2018 – 11/29/2018
Number of discharge measurements made	16	17

Precipitation monitoring

Twelve rainfall monitoring sites were identified that provided both access (landowner permission) and a spatially representative arrangement in and around four target subwatersheds (Figures 1 and 6; Table 4). Sites were also assessed for suitable physical characteristics that reduce impacts of wind and surrounding trees/buildings that may hinder the catch efficiency of the rain gage. This includes installation of rim of gage within 3-5 feet of the ground, and in a location where the distance-to-height ratio of surrounding objects is ideally 2:1, or at a minimum 1:1. Rain gages were 6-inch aluminum tipping bucket style with instantaneous logging of tips indexed to date and time. Representative photos are provided in Figure 6. The WC3 site was not established until the 2018 season due to administrative delays in equipment purchasing. The SC2 site was abandoned for 2018 after repeated instances of damage with unknown sources and discovery of complete destruction of tripod during the winter preceding the 2018 season.

Table 4: Rain gage locations

Site ID	Latitude (DD)	Longitude (DD)
NFEC1	43.8287	-73.3219
NFEC2	43.84523	-73.3136
NFEC3	43.81704	-73.2899
SC1	43.8994	-73.3714
SC2	43.9212	-73.3387
SC3	43.8842	-73.3587
WBDC1	43.9768	-73.3648
WBDC2	43.9575	-73.3652
WBDC3	43.9416	-73.3651
WC1	44.0312	-73.3989
WC2	44.0273	-73.3707
WC3	44.0543	-73.3747



Figure 6: Examples of rainfall gage sites at a) NFEC3, b) NFEC2, c) WC1, and d) WBDC1.

Each tipping bucket gage was tested for accuracy prior to the 2018 season using drip tests of known volume. Tipping mechanisms were adjusted accordingly until manufacturer’s stated accuracies were achieved. All instantaneous data underwent QA/QC review, comparing with neighboring gage data and regional weather data to filter out instances of erroneous tips or invalid periods of time resulting from clogged funnels or vandalism from human, avian, or bovine interference. These instances were rare. Gages were visited approximately twice monthly to offload data, check and correct levels and clean if needed.

QA/QC’d instantaneous data were resampled into 15-minute time-series of rainfall depth, and periods of likely snow accumulation and melt on the gage flagged with the help of temperature data and the National Operational Hydrologic Remote Sensing Center Interactive Snow Information dataset (NOHRSC, 2019). These days were replaced with daily depth of precipitation data from the PRISM dataset (PRISM, 2019), though they represented a very small portion of the record. 15-minute time-series data were summarized into both local calendar day totals as well as UTC day totals for use with the hydrologic model.

Water quality sampling

Seven stream locations were sampled in subwatersheds of the McKenzie Brook HUC-12 watershed in Addison County (Figure 1 and Table 1). Key site selection criteria included: local land-use dominated by agriculture, high likelihood of perennial streamflow, and site accessibility (i.e., landowner permission). These conditions allowed us to estimate phosphorous loading and establish a reference point for water quality conditions in subwatersheds of the McKenzie Brook Watershed.

Sampling targeted both dry- and wet-weather water quality, covering a range of streamflow, including 6 higher flow events at flow monitoring stations and samples of the rising limb of storm flow hydrographs. For these purposes, a high flow sampling event was coordinated in response to forecasted or observed rainfall events of 0.5 inches or more.

Table 5: Data Completeness in 2017 and 2018.

	Type of Sample/ Parameter	# of Actual Samples/ Year (Primary + QC)	# of Anticipated Samples/ Year (Primary + QC)	Sampling Frequency ^A	Sampling Method
Chemical	Total and Dissolved Phosphorus	2017 = 342 ^B 2018 = 281	284	Every 7-14 days (May 2 nd – Nov. 29th)	Grab

(A) – See EPA water quality monitoring QAPP Table 5 for details.

(B) Sampling began at the 5 water quality chemistry sites before the May 23rd start date, which accounts for actual sample numbers exceeding the anticipated number.

Laboratory QA/QC

Samples collected reflect conditions of individual waterbodies and tributaries in Vermont. To ensure representativeness, all samples were collected, preserved, and analyzed according to the procedures in the QAPP for this project, and within the specified holding times. Those results not meeting the project quality objectives of this program were flagged and reviewed to determine if appropriate quality controls were in place. Specifically, when two values had an RPD \geq 30%, the values were not considered to be within precision standards (Table 6).

Table 6: VAEL Laboratory analysis protocols for water samples

Parameter	Reporting Limit ^A	Accuracy ^B (% Recovery)	Estimated Precision for Field Duplicates ^C (RPD)	Laboratory Precision (RPD)	Analytical Method Reference ^B
Total and dissolved phosphorus	5 µg/l	85-115%	≤30%	15% ^B	<i>Std. Methods</i> (21 st ed.) 4500-P H. VAEL SOP 1.6, Rev. 6-2016

(A) - Reporting Limit is the minimum reported value (lowest standard in calibration curve or MDLx3)

(B) – VAEL SOP, Quality Assurance Manual Rev.15-2013.

(C) - Generated by the analysis of field duplicates

Table 7: Quality Control Completeness in 2017 and 2018.

	Parameter	
	TP (2017, 2018)	DP (2017, 2018)
Total # of samples	192, 140	150, 141
Total # of Field Duplicates	24, 19	20, 20
% of Field Dups (Goal is ≥10%)	12.5%, 13.5%	13.3%, 14.2%
Total # of Field Blanks	22, 11	18, 10
% of Field Blanks (Goal is ≥10%)	11.4%, 7.9% ^A	12%, 7.1% ^A

(A) Both parameters failed to meet the QC goal of 10% for field blanks in 2018 - Quality Control Completeness.

Rainfall-runoff model for ungaged sampling sites

To calculate streamflow and nutrient loading throughout the study area streamflow was modeled for the ungaged water quality sampling sites, except the lower NFEC0.7 site for which a simple drainage area adjustment was applied to the upstream observed daily flows at NFEC2.2. A spreadsheet runoff model was developed based on that put forth by Limbrunner et al. (2005). This semi-distributed continuous watershed model runs on a daily time step and employs the curve number method originally developed by the Soil Conservation Service (now NRCS) for small agricultural watersheds. The model can be constructed with readily available spreadsheet software, includes a subsurface soil-water accounting method with a simple channel storage routing feature, and can be implemented with only four adjustable parameters calibrated against observed data. These parameters are a snowmelt rate coefficient, curve number scaling factor, baseflow recession constant and a streamflow routing coefficient. Calculations can be summarized into the five equations listed below (Eq. 3 – 7*), with slight modifications to the streamflow and channel storage equations and addition of some parameters and variable constraints to maintain realistic ranges of values. See Limbrunner et al. (2005) for a complete description of model equations. Requiring minimal inputs of watershed characteristics, for each soil-landcover type it partitions effective precipitation into evapotranspiration, infiltration into the subsurface (in both the unsaturated shallow zone and deeper saturated groundwater) and runoff, then routes into streamflow on a daily time step using the Coordinated Universal Time (UTC) day (24-hour period ending 12:00 UTC).

$$\text{Infiltration: } I(t) = Pe(t) - R(t) \quad \text{Eq. 3}$$

$$\text{Unsaturated soil zone storage: } S(t) = S(t-1) + I(t) - Perc(t) - ET(t) \quad \text{Eq. 4}$$

$$\text{Saturated groundwater storage: } G(t) = G(t-1) + Perc(t) - k_b G(t-1) \quad \text{Eq. 5}$$

$$\text{Streamflow: } Q(t) = k_N N(t) \quad \text{Eq. 6}$$

$$\text{Channel storage: } N(t) = N(t-1) + R(t) + k_b G(t) - Q(t-1) \quad \text{Eq. 7}$$

*Where Pe = is effective precipitation taking into account snowmelt, R is direct runoff, $Perc$ is percolation from soil moisture compartment to deeper groundwater, ET is evapotranspiration, k_b is groundwater routing coefficient, k_N is channel storage routing coefficient, and Q is streamflow.

Daily streamflow was modeled for each sampling site's contributing area, as defined topographically in geographic information system software from a 0.7 meter LiDAR digital elevation model (Vermont Center for Geographic Information, 2016). Daylight hours data to estimate potential evapotranspiration using the Harmon method (Harmon, 1960) were downloaded from the U.S. Naval Observatory website (U.S. Naval Observatory, 2019) and daily temperature data from the PRISM climate data set (PRISM, 2019). Daily PRISM data represent the 24-hour period ending 12:00 UTC which necessitated the model's daily time step to run on the UTC day. All 15-minute streamflow, precipitation, and time-of-sample data were summarized into the UTC day. The model is a semi-distributed hydrologic model whose equations aggregate runoff for individual soil-land cover classes and rely on curve numbers assigned to each class. Runoff response for a given individual soil-land cover class was lumped and modeled as a unit, though its distribution throughout a subwatershed was not necessarily spatially contiguous. Curve numbers were estimated from the University of Vermont Spatial Analysis Lab's 2016 land cover dataset (UVM, 2019) and the Vermont USDA Natural Resource Conservation Service Top20 soils dataset (USDA-NRCS, 2016). Land cover and hydrologic soil group (HSG) data were each resampled in geographic information system software to get a 0.7-meter HSG raster (8 groups) and a 0.7 meter land cover raster (16 categories). These were then overlaid to produce a third raster that was coded to represent the specific HSG-land cover combination for each grid cell. Total area of each unique HSG-land cover combination within each subwatershed was calculated and those accounting for greater than 1 percent of the total subwatershed area were explicitly modeled and assigned a curve number using NRCS guidance (USDA-NRCS, 1986) and input from the local UVM Extension office. Areas of emergent vegetation, surface water, roads and other impervious were also classified and modeled separately regardless of percent coverage. The remaining areas of unique HSG-land cover individually making up less than 1 percent of the subwatershed were aggregated into a single classification unit with an area-weighted curve number. This land cover classification process produced a range of 10 to 14 different HSG-land cover modeling units, depending on the subwatershed. Actual evapotranspiration was also calculated and applied separately for each HSG-land cover unit.

Precipitation was driven by UTC daily watershed average rainfall, derived from 0.7-meter rasters of observed total precipitation for each day of the study period over the entire McKenzie Brook study area. Observed daily rainfall totals from the tipping bucket rain gages were interpolated via inverse distance squared weighting, the same routine employed by the PRISM dataset (PRISM, 2019) although with no elevation dependence due to the small elevation range of the study area. Other weighting exponents (e.g., 1 or 3) showed no improvement in a leave-one out validation test against observed data.

The runoff model produced modeled UTC daily streamflow from April 1st through November 30th and included a one-month spin-up period for each year beginning March 1st. The calibration dataset utilized calendar year 2018 data from the WBDC1 subwatershed, with model validation on WBDC 2017, NFEC 2017 and NFEC 2018 observed daily flows. The parameter set was calibrated to optimize the Nash-Sutcliffe Efficiency performance metric (NSE), and further adjusted subjectively considering metrics of percent bias (PBIAS) and ratio of the root mean square error to the standard (RSR) as

recommended in Moriasi et al. (2007). Watershed model performance is considered satisfactory if $NSE > 0.50$, $RSR \leq 0.70$ and if $PBIAS \pm 25\%$ (Moriasi et al., 2007). Original calibration for a single parameter set applied to an entire year (or both years) showed significant seasonal variation in model residuals. Stratifying the model into seasonal parameter sets provided substantial improvement in model performance. This may be due to the significant seasonality of such an agriculturally dominated landscape where a vast majority of the watershed experiences heavy land-use management and distinct periods of pre-, post-, and active growing season. Three seasons were defined subjectively as April 16th – May 15th, May 16th – September 30th, and October 1st – November 30th. Each year the April 1st through April 15th period included area-wide snowmelt events, which produced remarkably consistent unit-area runoff when comparing WBDC and NFEC flows, however were poorly represented by the model's snowmelt runoff algorithms. As such, during this period simple drainage area ratio extrapolation was applied to ungaged subwatersheds based on proximity to observed data. The final parameter sets with model calibration and validation statistics are presented in Tables 8 and 9, with modeled vs. observed hydrographs in Figure 7.

Table 8: Calibrated runoff model parameter set

	Pre-growing season	Growing season	Post-growing season
Calibrated streamflow routing parameter, k_N	0.503364	0.730000	0.316673
Calibrated baseflow recession constant, k_b :	0.757802	0.991823	0.000933
Calibrated CN scale factor, B	1.045199	1.010000	0.993383
Meltrate parameter, M :	0.600000	0.600000	0.600000

Table 9: Model calibration and validation statistics

	WBDC 2018 (calibration)	WBDC 2017 (validation)	NFEC 2017 (validation)	NFEC 2018 (validation)	Acceptability Criteria
NSE	0.68	0.63	0.76	0.90	>0.50
PBIAS	-18.65	20.57	-12.26	-2.98	$\pm 25\%$
RSR	0.57	0.60	0.49	0.32	≤ 0.70

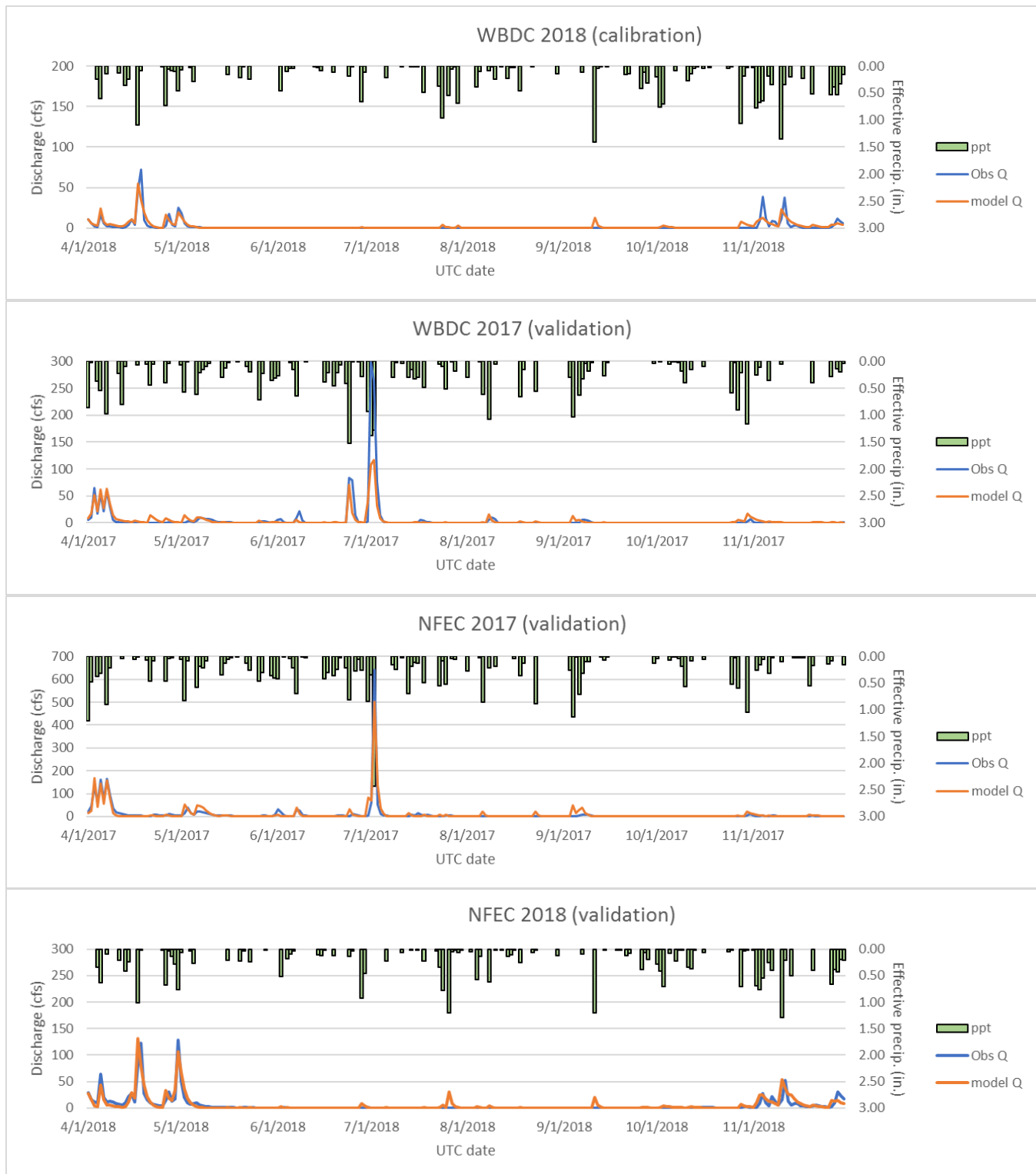


Figure 7: Runoff model calibration and validation hydrographs

Calculation of nutrient loads

Expressed in units of mass per unit time, nutrient flux for a stream is calculated by taking the product of observed (or modeled) streamflow and observed (or modeled) concentration of a solute. It is the rate a mass passes a point of interest for a given unit of time. This unit of time can vary and could be annual, daily or even sub-hourly depending on data availability and goals of a nutrient loading study. To characterize nutrient load over a longer period of interest, load is the integration of a series of individual concentration and streamflow data points as given by the following equation:

$$Load = k \int c(t)q(t)dt$$

where c is concentration for time t in ppb or $\mu\text{g/L}$, q is discharge for time t in cubic feet per second and k is a conversion factor to express loading in desired units, such as pounds per day. Because practical monitoring methods limit our ability to directly measure nutrient flux continuously, loading must be estimated using periodic observations. There are a variety of methods for estimating nutrient load for a period of interest using irregular or incomplete time-series of concentration and streamflow data. Each method has its own set of assumptions that should be considered for appropriate application. Resulting loads can vary depending on which method is utilized as well as additional factors like sampling frequency and timing, the quality of streamflow datasets and various seasonal dynamics in the hydrologic and biogeochemical systems. Three commonly applied techniques (Richards, 1998; Meals et al., 2013; Aulenbach et al., 2016) were considered for calculating nutrient loading for the McKenzie Brook monitoring project: a concentration-discharge regression model, the Beale Ratio Estimator, and what has been referred to in some studies as the Composite Method (Aulenbach and Hooper, 2006; Appling et al., 2015). To analyze the nature of our monitoring data and decide on the most appropriate method Microsoft Excel, the statistical software package SigmaPlot, and U.S. Army Corps of Engineers' FLUX32 software program were used. FLUX32 was then used to arrive at final estimates of nutrient loads at each water quality sampling site.

Regression models exploit correlations of continuous variables with measured solute concentrations (e.g., a discharge-concentration relationship) to estimate concentrations at time steps between sampling events and then construct a complete dataset of loading over time. This approach requires a sampling regime that covers a large range of observed flows in order to develop a well-defined concentration vs. flow relationship, that the correlation between discharge and measured solute concentrations is strong, and that there be low serial-correlation in the observed concentrations. The regression approach is able to produce a daily time-series of loading. For this study "Method 6" of the FLUX32 loading software was used, a regression approach that includes a bias correction step (Soballe, 2017).

The Beale Ratio Estimator calculates a flow-adjusted mean daily flow that is then multiplied by the number of days in your period of interest to arrive at a total mass load. A mean daily load is calculated from the individual loads of each sampling day. A flow adjustment factor is then applied by multiplying this value by the ratio of average flow for your entire period over average flow for your sampling days only. A bias correction factor is also applied. The Beale Ratio Estimator has been shown to be robust even in violation of assumptions and has outperformed other methods in some studies (Meals et al., 2013; Richards, 1998), however it only provides a total mass load for the period of interest.

The Composite Method is a hybrid of regression and a period-weighted approach. Sampling data are used to derive a linear regression model to estimate a continuous time-series of concentrations. For sampling days, the residuals of the observed and modeled data are then analyzed to extract correction factors that force modeled data points to equal observed values. A temporal interpolation of correction factors is used to create a continuous time-series of correction factors that is then applied to the modeled daily flows to arrive at a continuous time-series of corrected concentrations for use with daily streamflows to calculate daily loading. As with the standard regression model approach, this is also able to produce a daily time-series of loading. The Composite Method requires a strong correlation in the concentration-flow relationship and low serial-correlation in observed concentrations. For interpolated residual correction to provide

an improvement to the model, this method also demands a high serial-correlation in residual concentrations over time (Aulenbach et al., 2016).

For this study a method that could produce valid time-series of daily TP loads was preferred, however the nature of our concentration-flow relationship suggested that a regression model approach or the Composite Method would not be appropriate. As evidenced in Table 9a-b, the correlations between TP concentration and flow were poor for all sites. Stratification by season, year, flow magnitude or hydrograph (rising/falling/steady flows) did little to improve the correlations and was inconsistent site-to-site and year-to-year. A review of residuals of the regression plotted over time revealed some degree of seasonality at most sites (Figure 8), though this again was not consistent from site-to-site or even from year-to-year for individual sites. Spearman rank order correlation coefficients showed serial correlation on both the lag-1 measured TP concentrations (high) and lag-1 concentration residuals (moderate). Serial-correlation in the residuals would have been useful in the Composite Method, however Aulenbach et al. (2016) suggest using either a Composite Method or regression model only when the coefficient of determination for the concentration-discharge relationship is greater than about 0.30. When this is not the case other methods are preferable to applying corrections based on poor model prediction within the Composite Method. Cochran (1977) offers a sample variance criterion for determining when a ratio estimator reduces uncertainty as compared with averaging estimates, which is reiterated in guidance of Richards (1998). Their 0.5 threshold was exceeded at all sites for both TP and DP. For these reasons we chose to apply the Beale Ratio Estimator to estimate TP loads. FLUX32 was used for calculations, which also produces results from the method #6 regression model as well as a version of the composite method that uses residual interpolation and a maximum interpolation window of 14 days. We've included them in this report for comparative purposes.

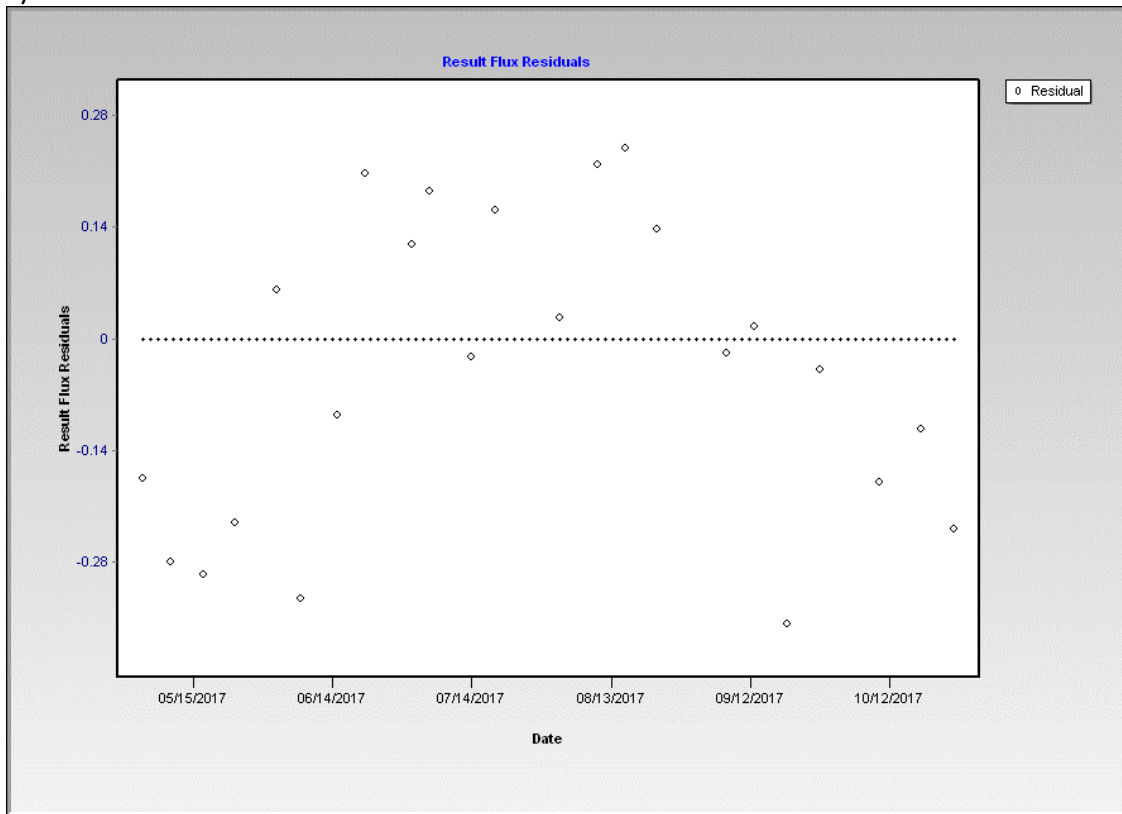
Table 9a: TP concentration-discharge regression results

Site	TP sample size (n)	R ²	Spearman Rank Order Corr. Coeff. On lag-1 conc.	Spearman Rank Order Corr. Coeff. On lag-1 residuals
NFEC0.7	42	0.29	0.668 (p < 0.00001)	0.475 (p = 0.00181)
NFEC2.2	41	0.15	0.556 (p = 0.000219)	0.461 (p = 0.00294)
Stony Crk	25	0.32	-0.522 (p = 0.806)	-0.263 (p = 0.212)
WBDC	30	0.00	0.594 (p = 0.000720)	0.594 (p = 0.000720)
Braisted Brk	38	0.26	0.169 (p = 0.314)	-0.0673 (p = 0.690)
Wards Crk	20	0.01	0.449 (p = 0.0527)	0.421 (p = 0.071)
Hospital Crk	25	0.22	0.275 (p = 0.191)	0.227 (p = 0.282)

Table 9b: DP concentration-discharge regression results

Site	DP sample size (n)	R ²	Spearman Rank Order Corr. Coeff. On lag-1 conc.	Spearman Rank Order Corr. Coeff. On lag-1 residuals
NFEC0.7	19	0.12	0.804 (p < 0.00000)	0.596 (p = 0.00704)
NFEC2.2	19	0.04	0.36 (p = 0.127)	0.346 (p = 0.144)
Stony Crk	7	0.44	-0.257 (p = 0.658)	-0.143 (p = 0.803)
WBDC	9	0.83	0.857 (p = 0.00178)	0.786 (p = 0.0149)
Braisted Brk	19	0.56	0.589 (p = 0.010)	0.311 (p = 0.205)
Wards Crk	5	0.25	1.00 (p = 0.0833)	0.800 (p = 0.333)
Hospital Crk	6	0.17	-0.600 (p = 0.35)	-0.600 (p = 0.350)

a)



b)

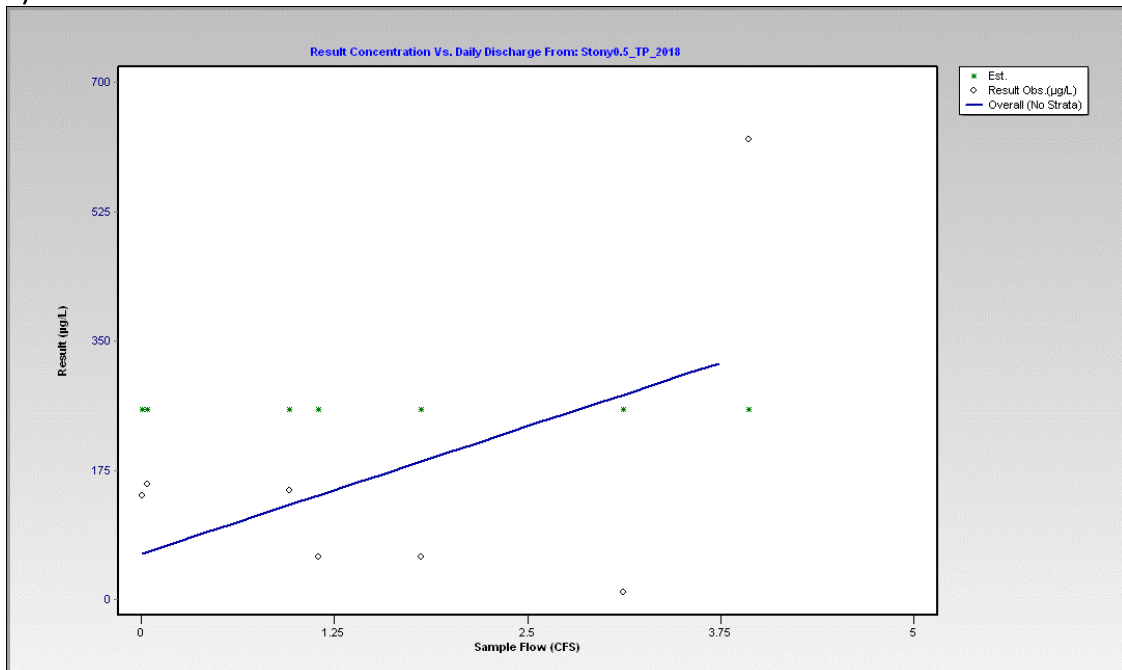


Figure 8: FLUX32 regression outputs of a) TP model residual over time for NFEC2.2 in 2017; and b) TP concentration-discharge relationship for Stony Creek in 2018. Green markers for Stony Creek are the modeled concentrations (a single daily average value from the Beale Ratio Estimator method).

Results

Precipitation

Table 10 presents a summary of monthly rainfall data for each target subwatershed. As you would expect, individual gage data were similar to adjacent gages with values diverging as a function of distance. Figure 9 shows that in general rainfall totals were above normal for spring and summer and normal to below normal in 2017. A significant rainfall event occurred on July 1, 2017 with NFEC1 logging 2.59 inches, approximately 2.0 inches of which fell in a two-hour period. This was the highest magnitude event of any gage for both years and impacted all subwatersheds, though northerly gages saw their 2017 daily maximum occur during an event a few days prior. The 2018 monitoring period proved to be much drier, with above normal April and November precipitation, but a persistent below normal period from May through September. There were some significant 24-hour event totals of approximately 1.5 inches in late July and early September. The complete data are included in an accompanying dataset available through the Lake Champlain Basin Program.

Table 10: Monthly rainfall totals (subwatershed average)

	Total precip. (in.)	NFEC0.7	NFEC2.2	Stony Crk	Braisted Brk	WBDC	Wards Crk	Hosp. Crk
2017	Apr	3.92	3.92	4.07	3.74	3.75	3.74	3.92
	May	4.5	4.5	4.53	4.12	4.12	4.54	4.5
	Jun	5.21	5.22	7.19	5.63	5.65	5.98	5.21
	Jul	6.04	6.04	6.48	5.4	5.44	4.92	6.04
	Aug	2.98	2.96	4.02	3.39	3.43	3.21	2.98
	Sept	2.84	2.84	2.97	2.89	2.88	3.12	2.84
	Oct	3.23	3.24	3.32	3.28	3.29	3.37	3.23
	Nov	1.7	1.69	1.72	1.61	1.6	1.52	1.7
2018	Apr	4.5	4.49	4.28	3.92	3.91	4.11	4.19
	May	1.1	1.09	1.08	1.03	1.03	1.05	1.1
	Jun	2.75	2.74	2.44	1.87	1.84	1.92	1.79
	Jul	3.04	3.04	3.44	3.4	3.4	3.65	3.78
	Aug	2.14	2.09	2.32	1.83	1.77	2.33	2.52
	Sept	2.16	2.18	2.77	2.73	2.74	2.87	2.88
	Oct	3.35	3.35	3.31	2.99	3	3.08	2.88
	Nov	5.58	5.59	5.71	5.69	5.65	6.05	6.02

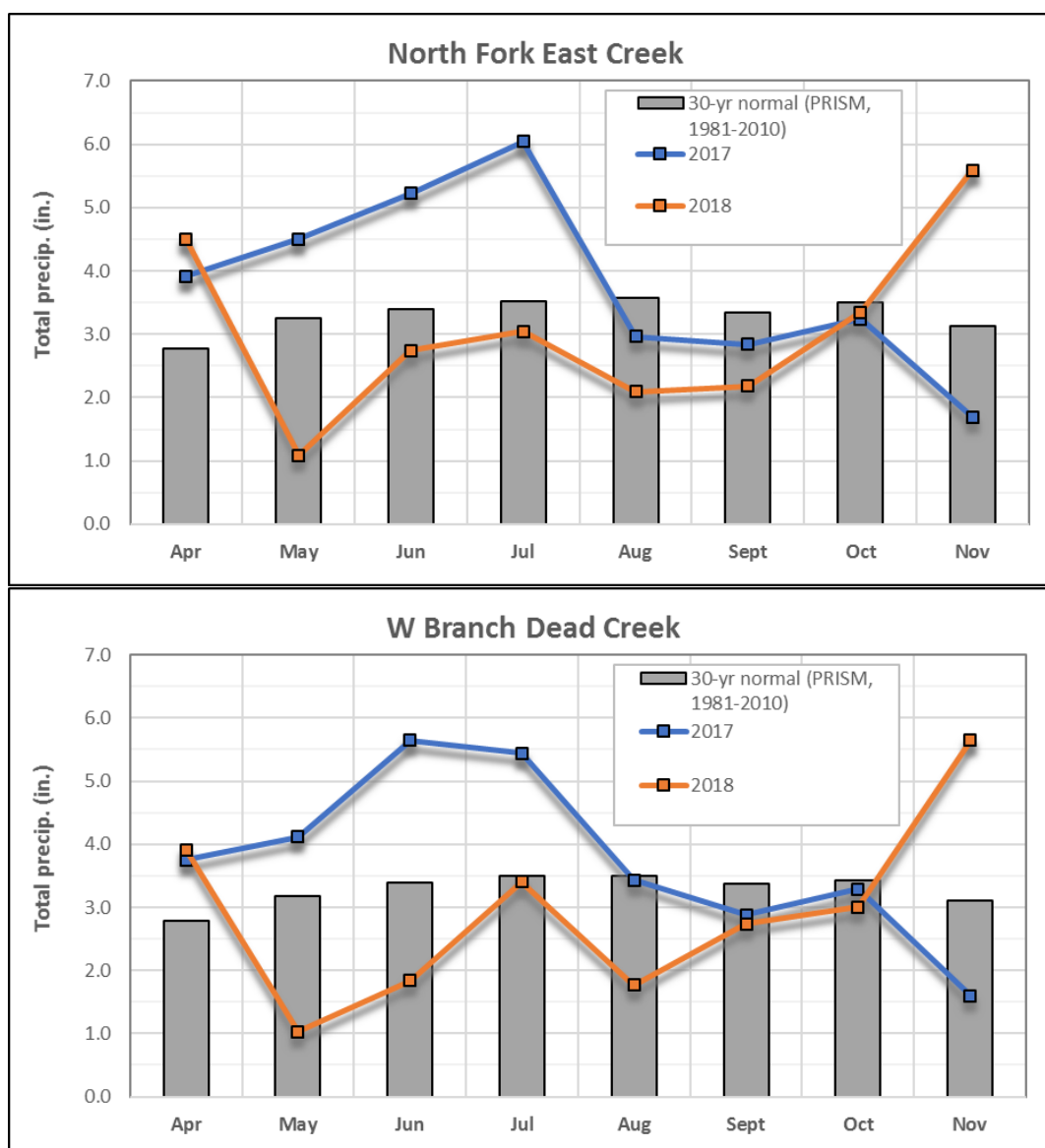


Figure 9: Monthly watershed average precipitation for the NFEC and WBDC subwatersheds during the study period.

Observed Streamflow

Figure 10 shows the calendar year 2017 and 2018 14-day average streamflow for the nearby USGS stream gage on Little Otter Creek against period of record normal flows. It echoes the rainfall data with a wet to very wet spring and summer and dry fall of 2017, and a very dry summer 2018. This pattern is reflected in the hydrographs for our two streamflow gaging stations, with a notable July 2017 event far greater than any other and a 2018 summer period where flows remained at or around 0 cfs for extended periods of time (Figure 11). Table 11 shows summary statistics based on mean daily discharges. The complete data are included in an accompanying dataset available through the Lake Champlain Basin Program.

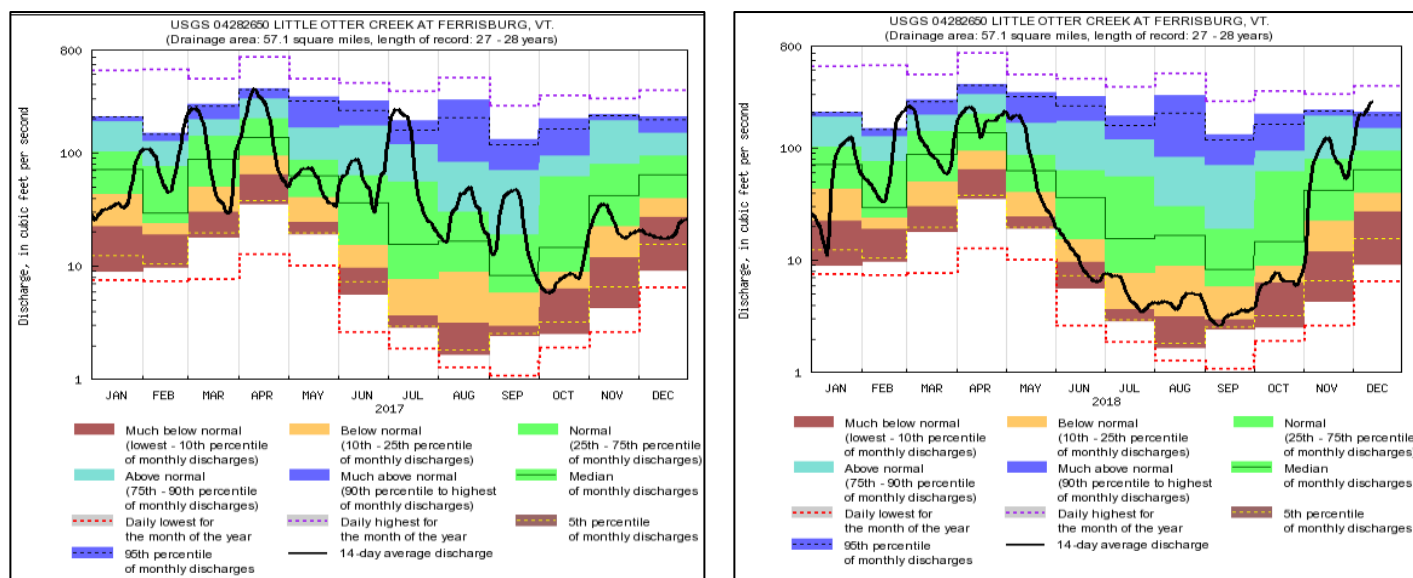


Figure 10: Calendar year 2017 and 2018 14-day average streamflow for the nearby USGS stream gage on Little Otter Creek against 28 year period of record.

Table 11: Summary statistics of observed daily streamflow at NFEC and WBDC gages.

WBDC Avg. Q (cfs)	2017	2018
Apr	9.2	8.7
May	2.1	1.1
Jun	7.7	0.0
Jul	21.6	0.0
Aug	0.8	0.0
Sept	0.5	0.0
Oct	0.4	0.1
Nov	0.1	6.0
Period avg.:	5.3	2.0
Max daily:	298.8	72.5
Min daily:	0.0	0.0

NFEC Avg. Q (cfs)	2017	2018
Apr	30.9	25.4
May	7.5	4.5
Jun	6.4	0.1
Jul	28.0	0.1
Aug	0.5	0.0
Sept	1.5	0.0
Oct	1.0	0.7
Nov	1.9	10.6
Period avg.:	9.7	5.1
Max daily:	641.4	128.5
Min daily:	0.0	0.0

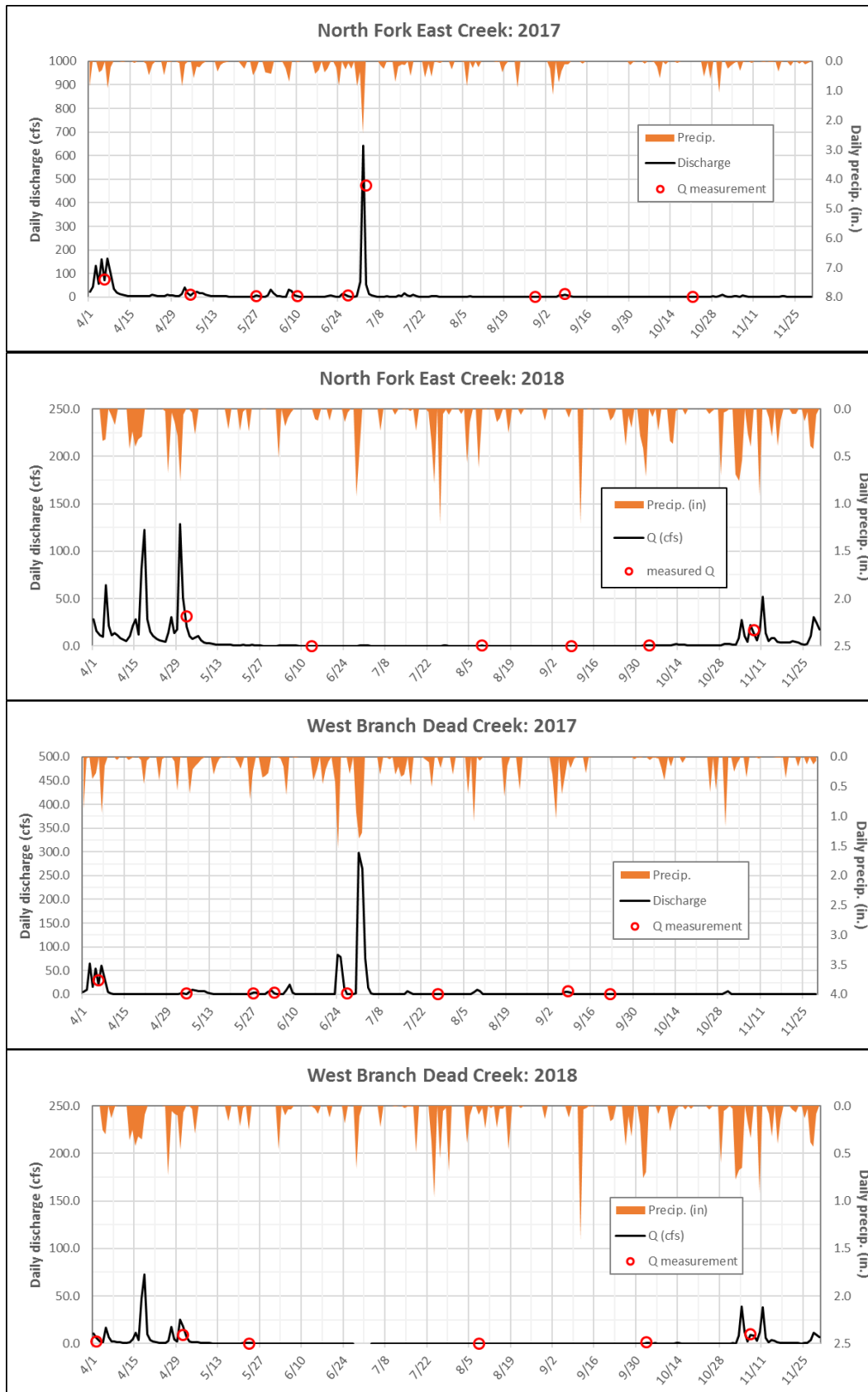


Figure 11: Hydrographs of daily mean discharge at NFEF and WBDC streamflow gages. Note that the 2017 high flow measurement is an indirect measurement method via the slope-area method.

Modeled Streamflow

Modeled streamflow hydrographs for the ungaged subwatersheds are in Figure 12. Summary statistics of modeled flows are presented in Table 11. The complete data are included in an accompanying dataset available through the Lake Champlain Basin Program.

Table 11: Summary statistics of modeled flows for ungaged sampling sites

Site (drainage area):	NFEC0.7 (12.3 mi. ²)		Stony Crk (1.4 mi. ²)		Braist. Brk (2.3 mi. ²)		Wards Crk (1.9 mi. ²)		Hosp. Crk (1.1 mi. ²)	
Avg. Q (cfs)	2017	2018	2017	2018	2017	2018	2017	2018	2017	2018
Apr	34.8	28.5	4.0	3.4	5.2	4.8	4.2	4.1	2.4	2.4
May	8.5	5.1	1.3	0.5	1.4	0.6	1.7	0.4	1.2	0.3
Jun	7.1	0.1	3.3	0.1	2.5	0.1	2.4	0.1	1.6	0.0
Jul	31.5	0.1	3.5	0.2	5.1	0.2	3.4	0.2	1.7	0.2
Aug	0.5	0.0	1.1	0.1	0.7	0.1	0.4	0.2	0.2	0.1
Sept	1.6	0.0	1.2	0.3	1.1	0.4	1.0	0.3	0.8	0.2
Oct	1.1	0.8	0.3	0.5	0.4	0.6	0.4	0.4	0.3	0.2
Nov	2.2	11.9	0.5	2.0	0.8	3.3	0.7	2.9	0.5	1.9
Period avg.:	10.9	5.8	1.9	0.9	2.2	1.2	1.8	1.0	1.1	0.7
Max daily:	721.2	144.4	50.8	18.9	66.5	30.8	41.8	25.3	20.4	14.8
Min daily:	0.0	0.0	0.0	0.0	0.0	0.0	0.0	0.0	0.0	0.0

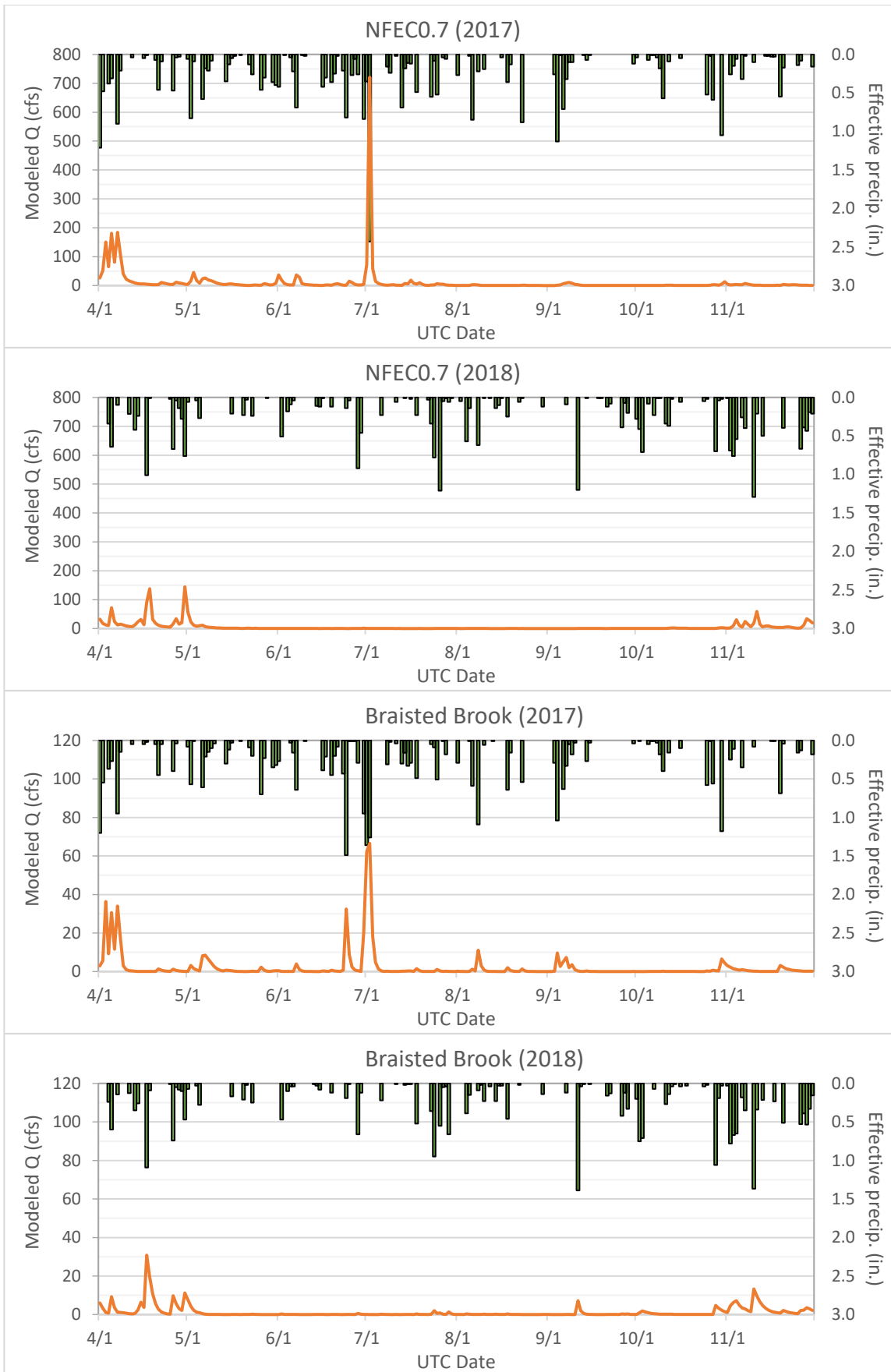


Figure 12: modeled streamflow for ungaged water quality sampling sites



Figure 12 cont'd: modeled streamflow for ungaged water quality sampling sites

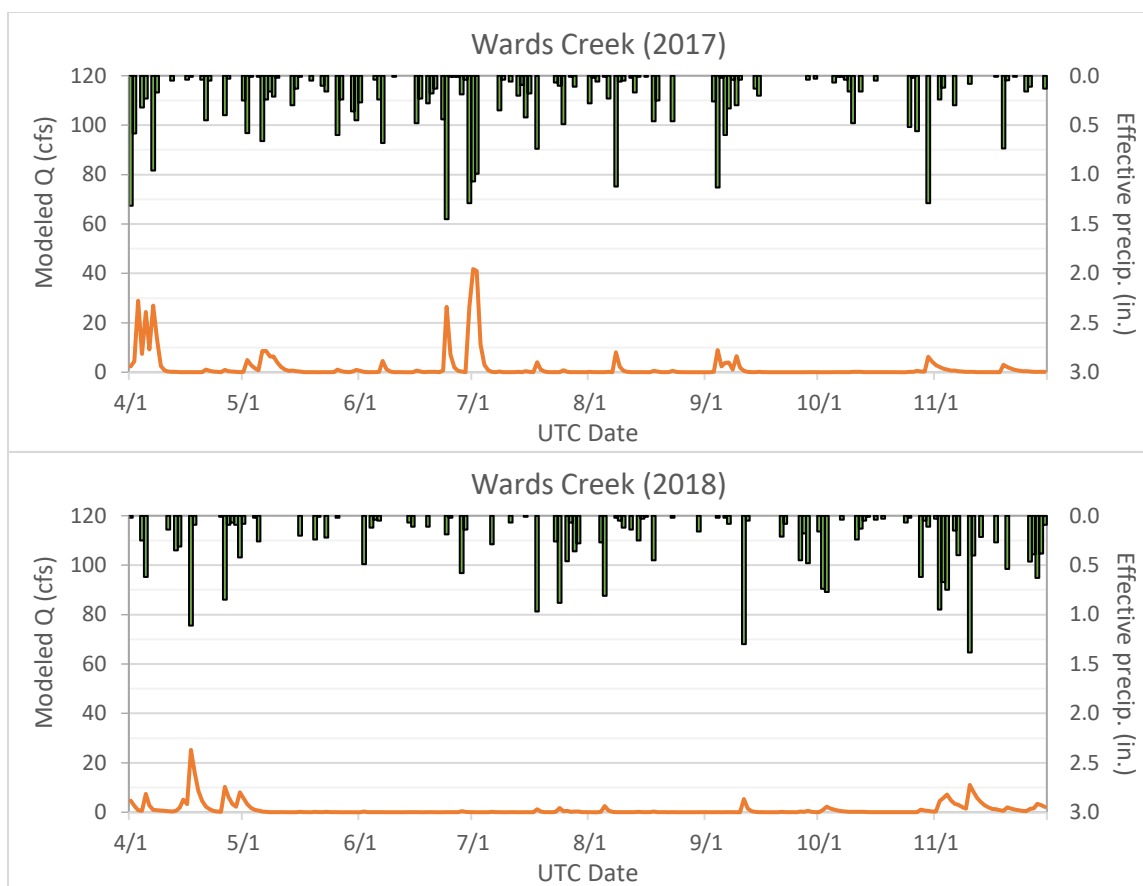
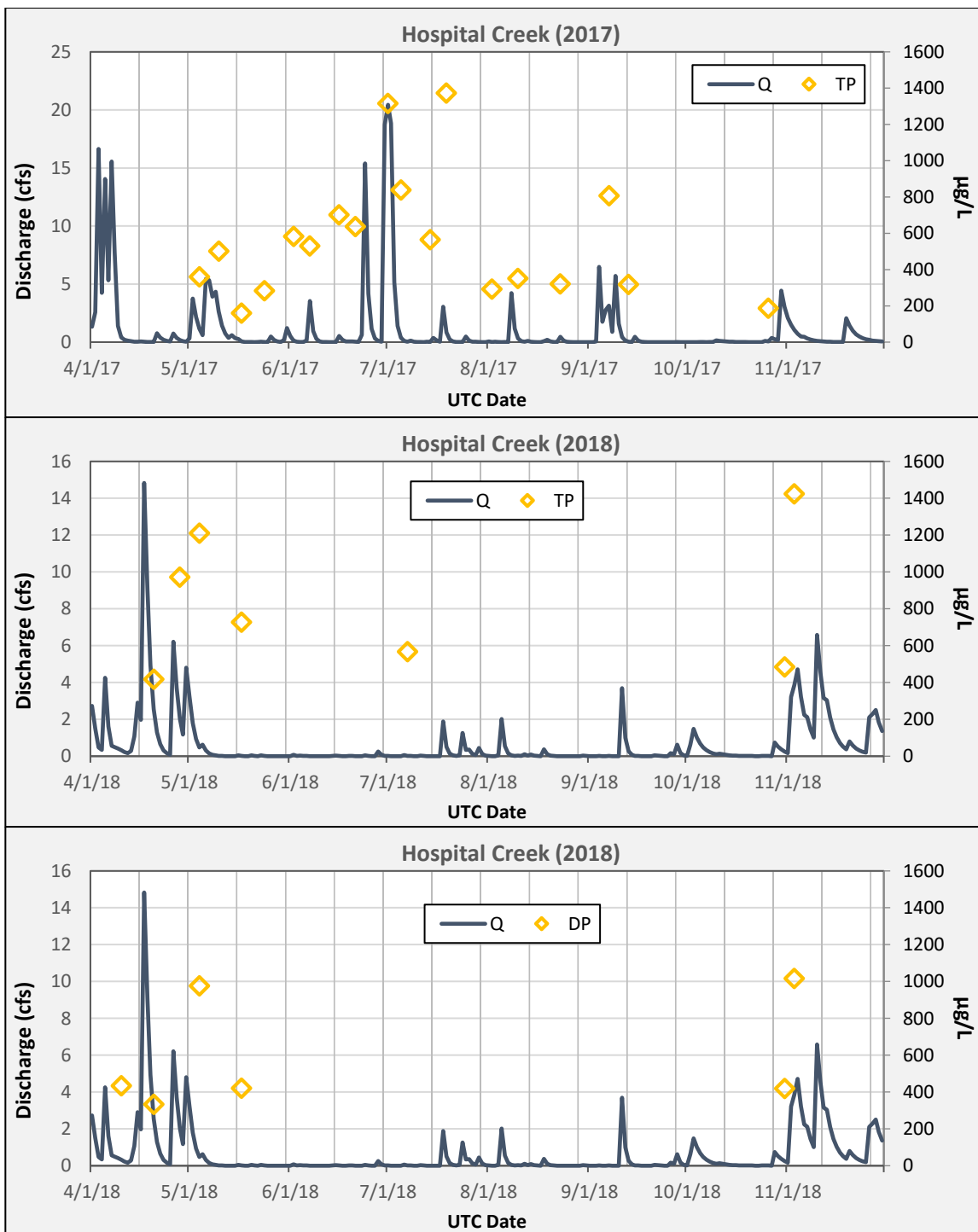
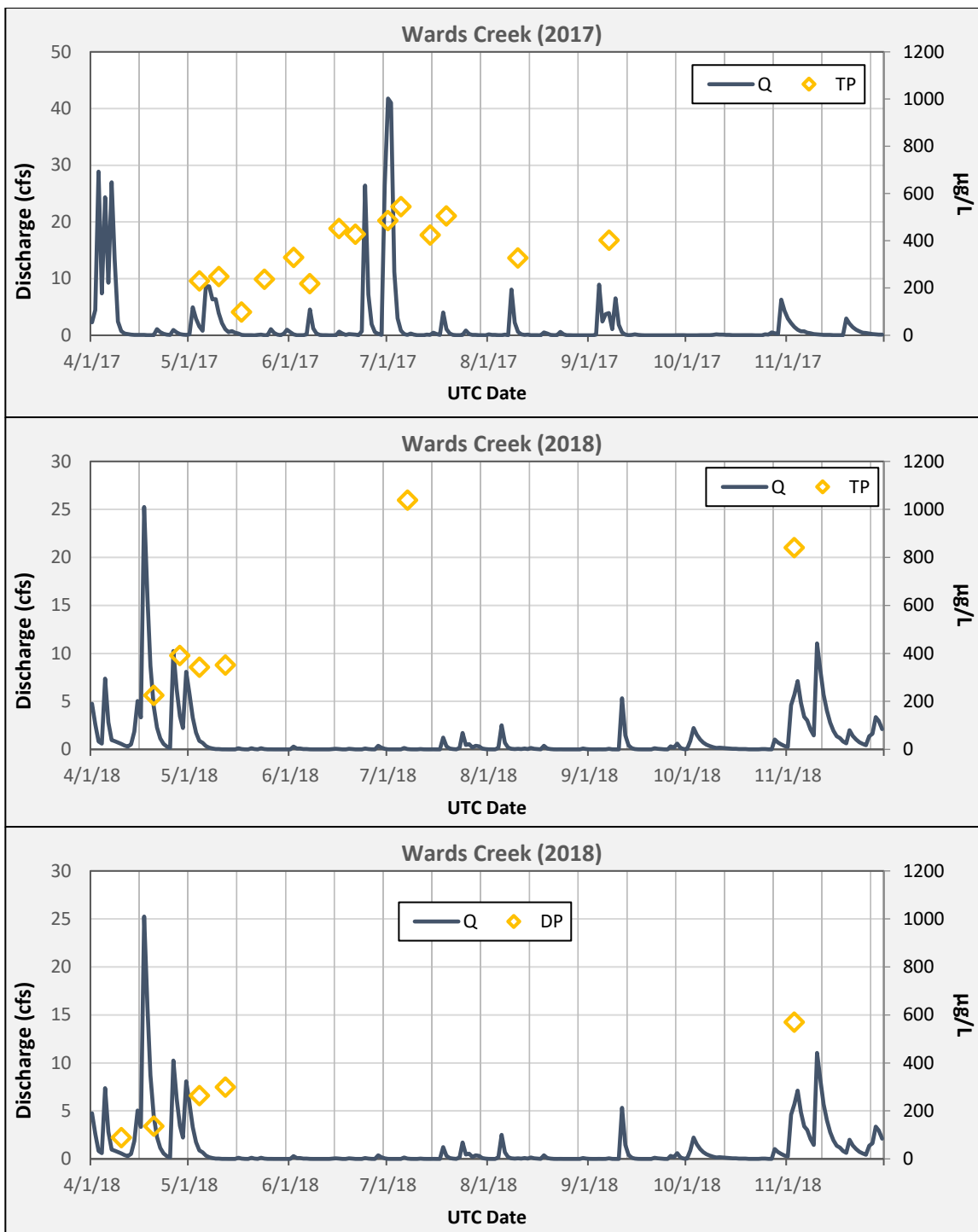


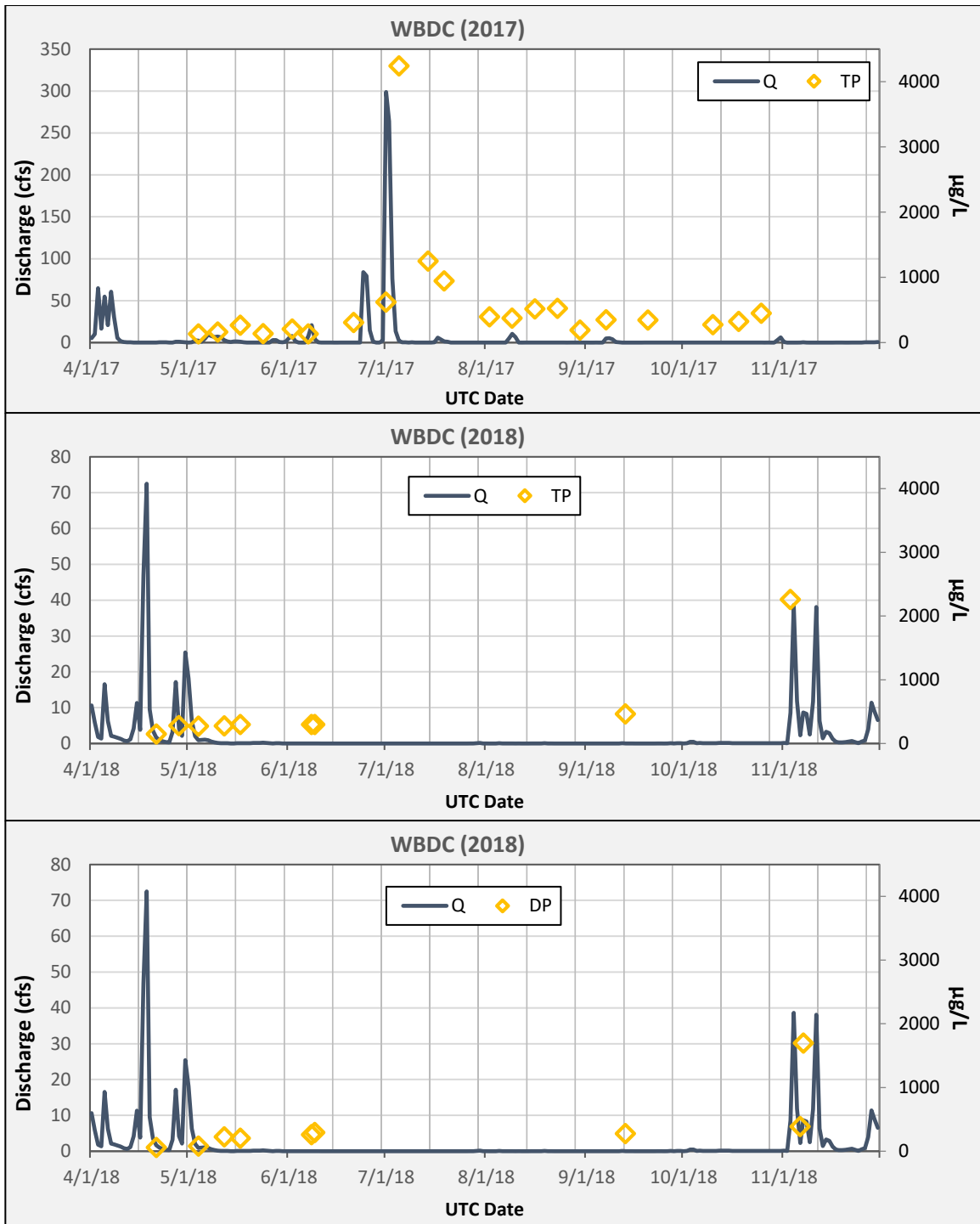
Figure 12 cont'd: modeled streamflow for ungaged water quality sampling sites

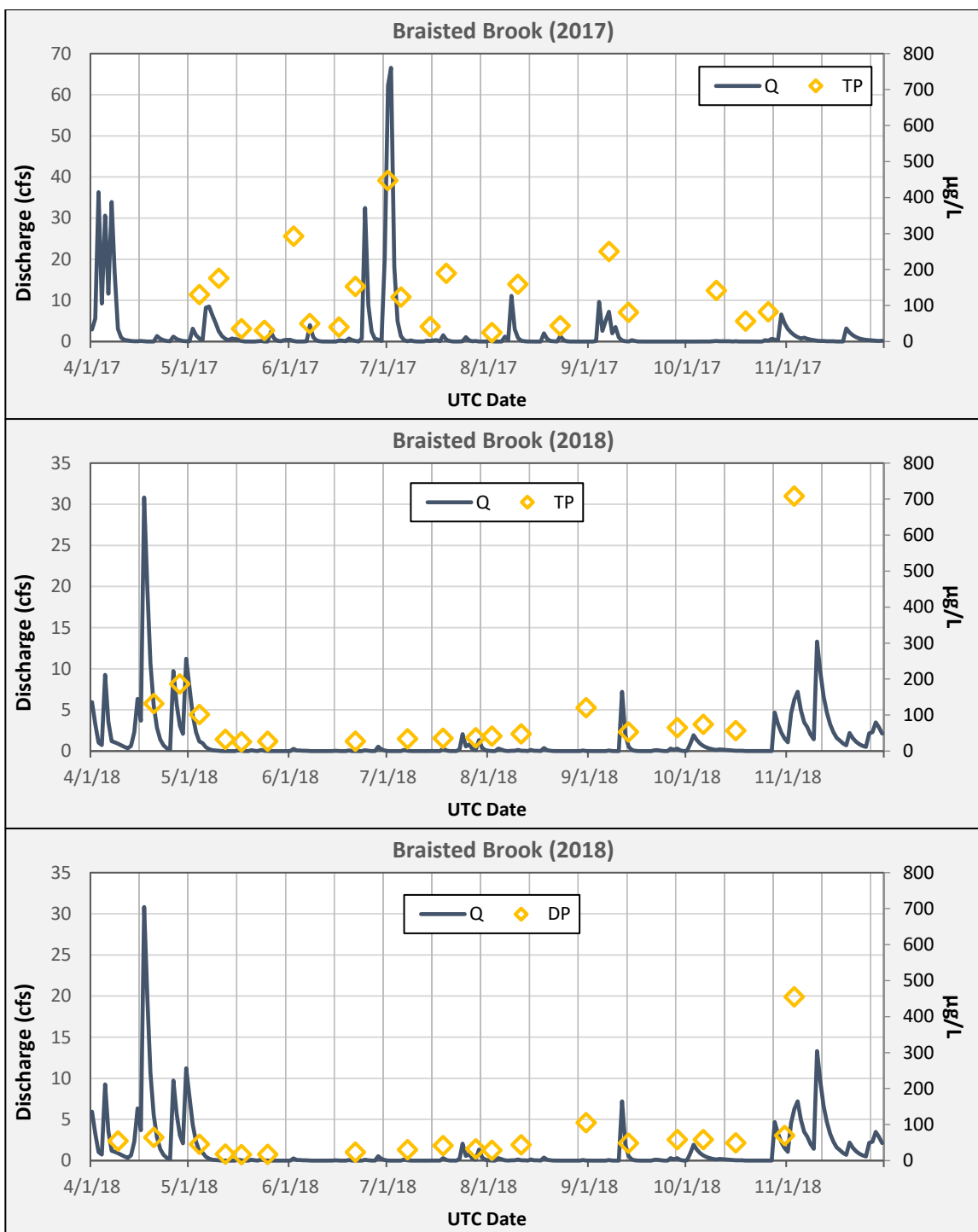
Water Chemistry

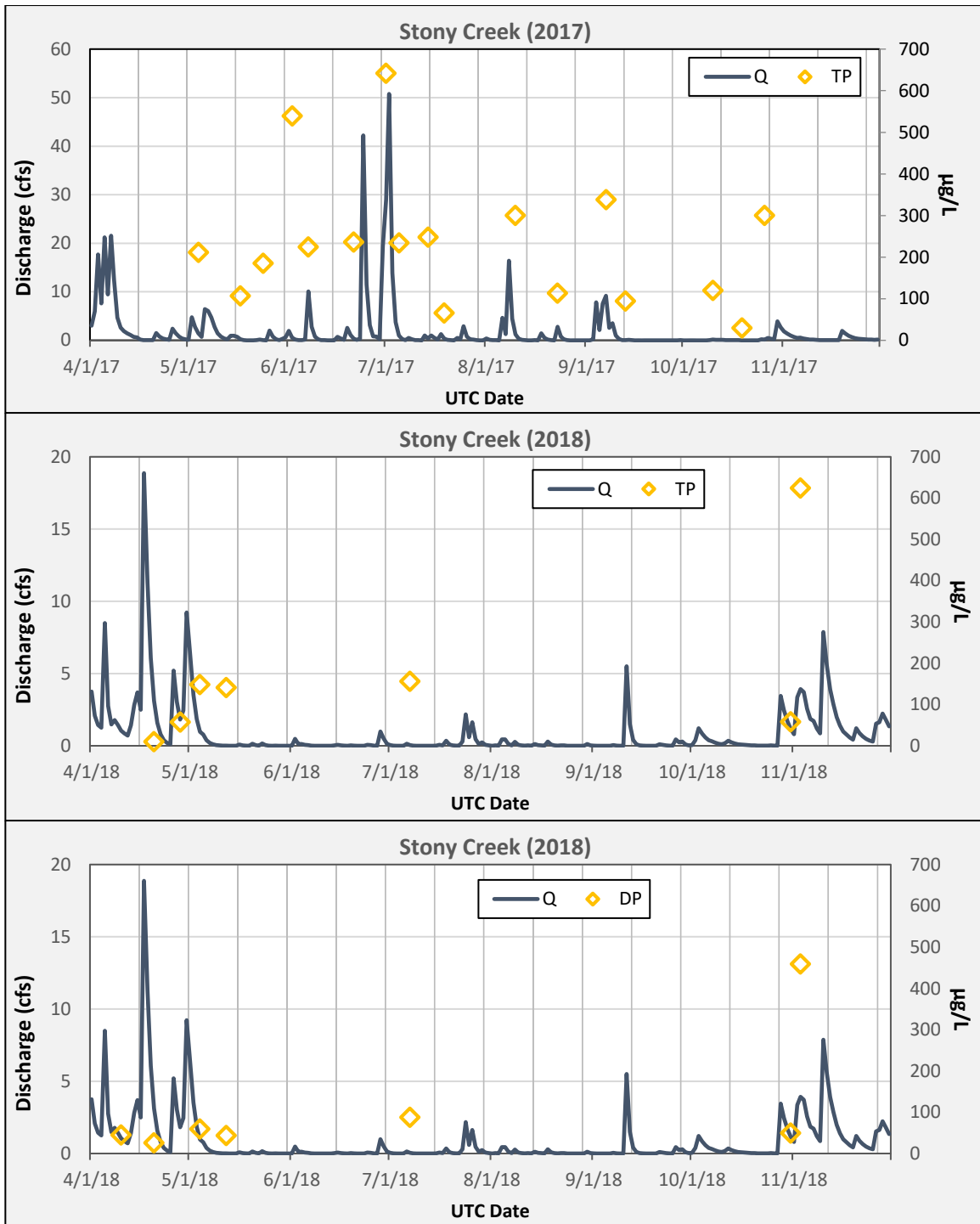
Measured total and dissolved phosphorous concentrations in $\mu\text{g/L}$ are plotting with streamflow for all sample sites in Figure 13 over the next seven pages. The complete data are included in an accompanying dataset available through the Lake Champlain Basin Program.

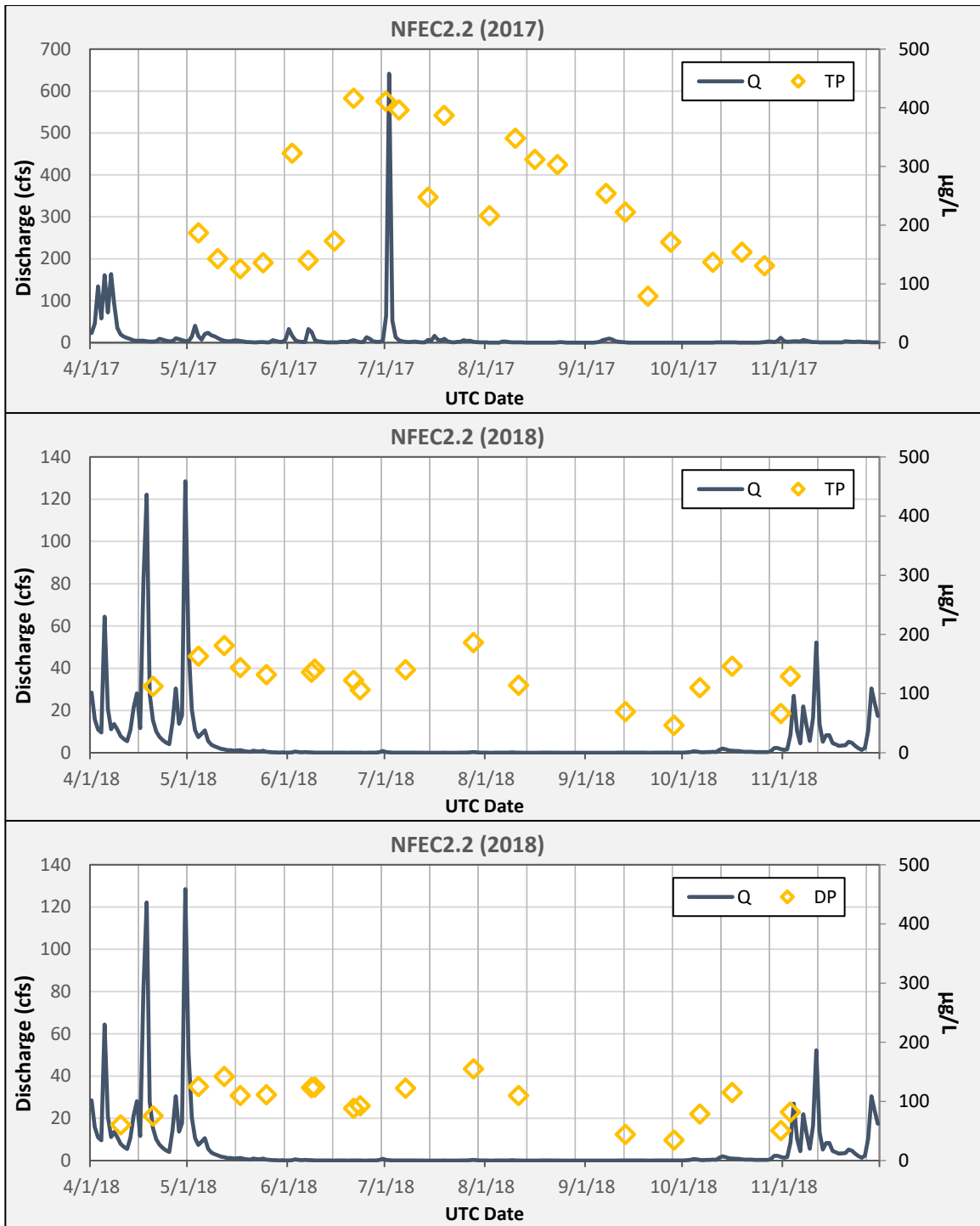












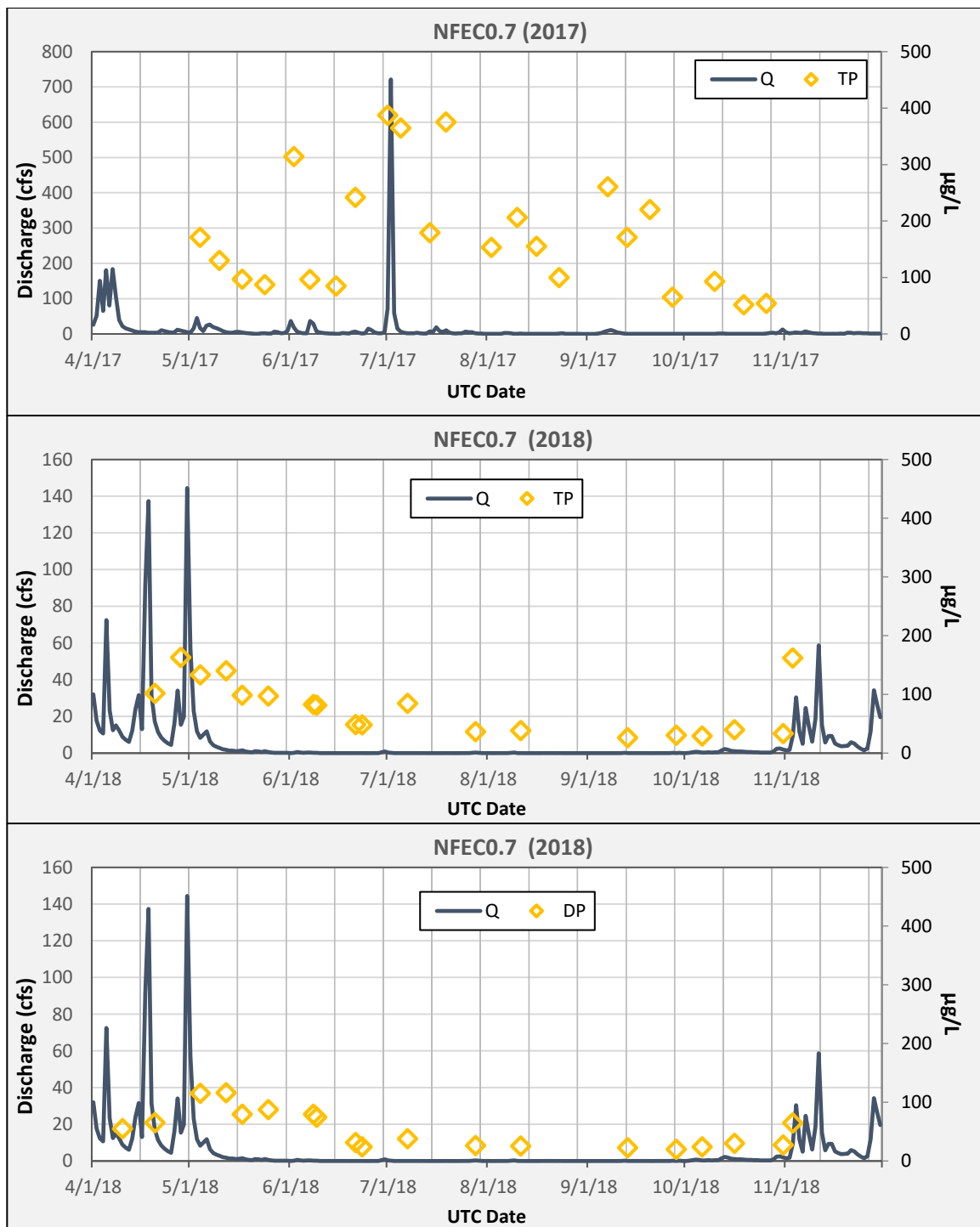


Figure 13: Total and dissolved phosphorous concentrations in µg/L are plotting with streamflow for all sample sites

Loading Calculations

The Beale Ratio Estimator with flow adjustment was deemed the most appropriate given guidance in the literature and the nature of the concentration-flow relationships. Results are compared with alternative methods in Table 12a-c. While the choice among different methods has some impact on resulting loads, the flow weighting step in the chosen approach has a substantial influence on results. This stems from the sometimes large difference in flows for sample days and that of the overall monitoring period. There was some positive correlation between concentrations and flows, (albeit weak), so the decision to adjust for this ratio was supported in that respect. In this case where discharge-concentration relationships are weak there is also value in sampling on days indicative of the flow for the entire period

even when using a method that give a single total load like the Beale Ratio Estimator, though this is obviously difficult to characterize ahead of time. Figure 14 shows TP and DP yields (lbs/acre) against specific period average flow (ft.³/s/mi.²) for each site.

Table 12a: Total phosphorous loads during 2017 study period, as calculated in FLUX32

		NFEC0.7	NFEC2.2	Stony Creek	WBDC	Braisted Brook	Wards Creek	Hosp. Creek
<i>Ave total Q (cfs)</i>		10.92	9.72	1.89	5.32	2.15	1.77	1.07
<i>Ave sample Q (cfs)</i>		9.13	8.12	3.35	16.43	4.10	4.24	1.88
Total Apr 1 - Nov. 30, 2017 TP loading (lbs)	Beale Ratio w/ flow adj (yield per acre)	4615.47 (0.59)	4552.2 (0.65)	560.88 (0.61)	1348.7 (0.5)	489.34 (0.33)	405.79 (0.34)	768.09 (1.12)
	Beale Ratio w/o flow adj	3763.07	3751.65	1134.14	4191.79	1072.96	1021.10	1476.55
	Regression	3732.10	3783.69	1106.46	3790.87	785.31	997.91	1273.83
	Regression w/ residual interp.	4215.35	4118.31	1141.29	4862.37	851.96	1004.80	1329.18
Flux rate (lbs/day)	Beale Ratio w/ flow adj	18.92	18.66	2.30	5.53	2.01	1.66	3.15
	Beale Ratio w/o flow adj	15.43	15.38	4.65	17.18	4.40	4.19	6.05
	Regression	15.30	15.51	4.54	15.54	3.22	4.09	5.22
	Regression w/ residual interp.	17.28	16.88	4.68	19.93	3.49	4.12	5.45
Flow wtd. conc. (µg/L)	Beale Ratio w/ flow adj	321.00	356.00	225.00	193.00	173.00	174.00	545.00
	Beale Ratio w/o flow adj	262.00	293.00	455.00	599.00	379.00	437.00	1048.00
	Regression	260.00	296.00	444.00	541.00	277.00	427.00	904.00
	Regression w/ residual interp.	293.00	322.00	458.00	694.00	301.00	430.00	943.00

Table 12b: Total phosphorous loads during 2018 study period, as calculated in FLUX32.

		NFEC0.7	NFEC2.2	Stony Creek	WBDC	Braisted Brook	Wards Creek	Hosp. Creek
<i>Ave total Q (cfs)</i>		5.75	5.12	0.86	1.97	1.24	1.05	0.66
<i>Ave sample Q (cfs)</i>		3.08	2.13	1.57	1.74	1.01	2.43	1.31
Total Apr 1 - Nov. 30, 2018 TP loading (lbs)	Beale Ratio w/ flow adj (yield per acre)	1997.28 (0.25)	2166.99 (0.31)	170.04 (0.18)	4046.73 (1.51)	702.31 (0.47)	318.59 (0.27)	422.14 (0.61)
	Beale Ratio w/o flow adj	974.91	869.74	291.58	3537.50	538.85	712.41	877.28
	Regression	958.30	993.98	229.41	1716.04	315.77	720.79	826.53
	Regression w/ residual interp.	975.76	940.36	187.84	1784.03	356.05	644.32	766.80
Flux rate (lbs/day)	Beale Ratio w/ flow adj	8.19	8.88	0.70	16.59	2.88	1.31	1.73
	Beale Ratio w/o flow adj	4.00	3.57	1.20	14.50	2.21	2.92	3.60
	Regression	3.93	4.07	0.94	7.03	1.29	2.95	3.39
	Regression w/ residual interp.	4.00	3.85	0.77	7.31	1.46	2.64	3.14
Flow wtd. conc. (µg/L)	Beale Ratio w/ flow adj	264.00	322.00	150.00	1564.00	431.00	231.00	486.00
	Beale Ratio w/o flow adj	129.00	129.00	257.00	1367.00	331.00	516.00	1011.00
	Regression	127.00	148.00	203.00	663.00	194.00	522.00	952.00
	Regression w/ residual interp.	129.00	140.00	166.00	690.00	219.00	467.00	883.00

Table 12c: Dissolved phosphorous loads during 2018 study period, as calculated in FLUX32.

		NFEC0.7	NFEC2.2	Stony Creek	WBDC	Braisted Brook	Wards Creek	Hosp. Creek
<i>Ave total Q (cfs)</i>		5.75	5.12	0.86	1.97	1.24	1.05	0.66
<i>Ave sample Q (cfs)</i>		2.74	2.44	1.47	1.41	0.92	2.33	1.25
Total Apr 1 - Nov. 30, 2018 DP loading (lbs)	Beale Ratio w/ flow adj (yield per acre)	1250.77 (0.16)	1221.8 (0.17)	128.81 (0.14)	4344.41 (1.62)	473.75 (0.32)	222.55 (0.19)	322.93 (0.47)
	Beale Ratio w/o flow adj	536.19	579.53	229.42	3105.57	329.02	495.62	642.25
	Regression	640.64	680.80	141.59	1133.77	191.55	435.77	621.42
	Regression w/ residual interp.	609.58	620.92	125.51	1047.02	200.81	388.23	579.10
Flux rate (lbs/day)	Beale Ratio w/ flow adj	5.13	5.01	0.53	17.81	1.94	0.91	1.32
	Beale Ratio w/o flow adj	2.20	2.38	0.94	12.73	1.35	2.03	2.63
	Regression	2.63	2.79	0.58	4.65	0.79	1.79	2.55
	Regression w/ residual interp.	2.50	2.55	0.51	4.29	0.82	1.59	2.37
Flow wtd. conc. (µg/L)	Beale Ratio w/ flow adj	165.00	181.00	114.00	1679.00	291.00	161.00	372.00
	Beale Ratio w/o flow adj	70.80	86.10	203.00	1200.00	202.00	273.90	740.00
	Regression	84.60	101.00	125.00	438.00	118.00	316.00	716.00
	Regression w/ residual interp.	80.50	92.20	111.00	405.00	123.00	281.00	667.00

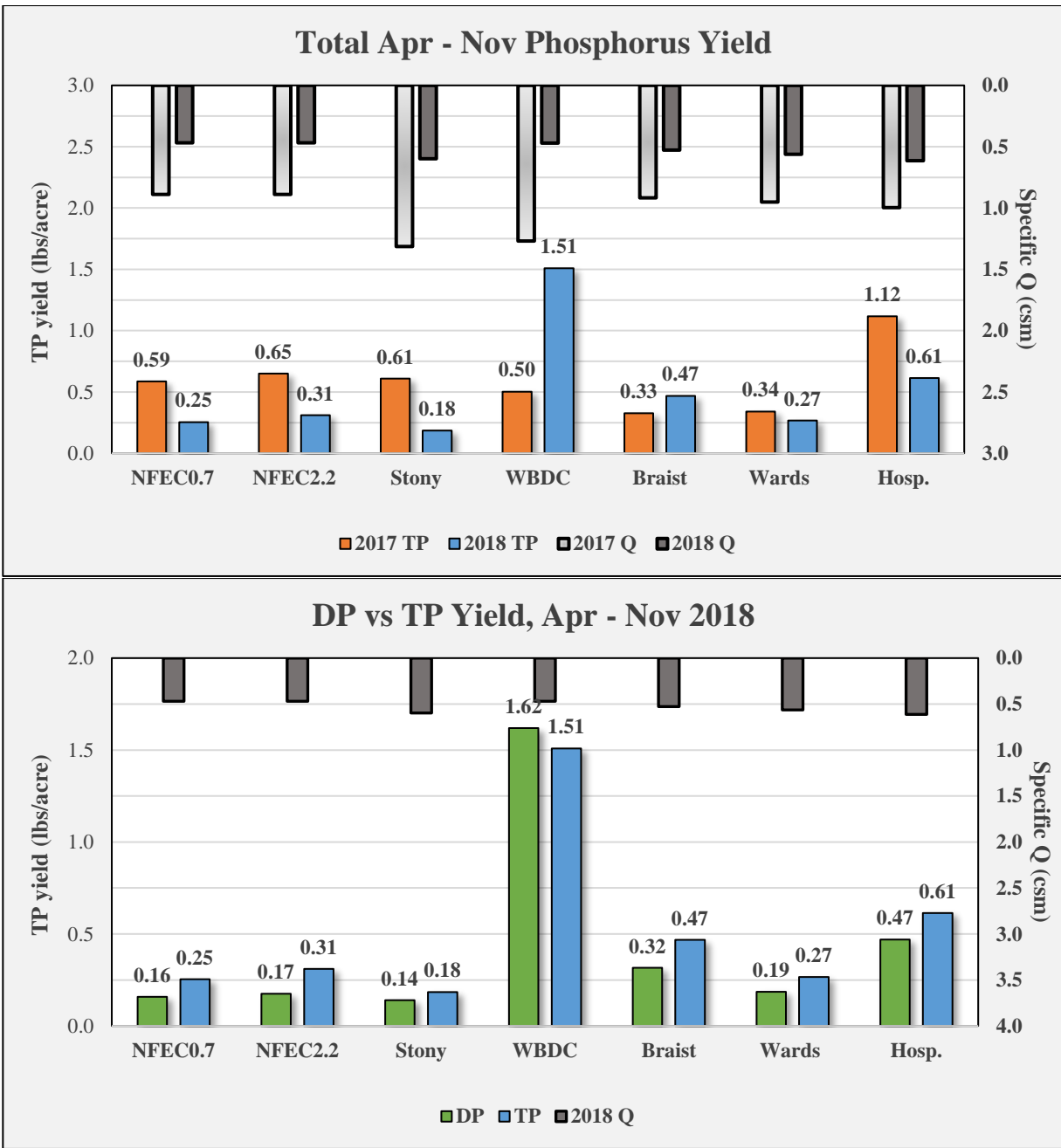


Figure 13: TP and DP yields with period average specific discharge for each site.

Sources of uncertainty

There are a multitude of sources of uncertainty in a complex and multi-faceted study like this one. From a hydrological perspective, the largest source of uncertainty in gaged flows is likely the extension of the rating curve to flows beyond those that have been directly measured, although applying a slope-area estimation is an improvement over simple extrapolation in the case of NFEC1. Additionally, changing hydraulics at WBDC1 with constant shifts in the rating introduce added and potentially substantial uncertainty to that time-series of rated streamflow. For modeled streamflow, there were no parameters or equations that specifically accounted for subsurface tile drainage behavior, nor would this information have been available even if a routine was added to address this. If ungaged watersheds have significantly different unaccounted for characteristics such as tile-drainage networks, modeled flows could be in

substantial error. Finally, beyond seasonally calibrated parameters the model does not have any information on impacts of management activities on the landscape which may vary from subwatershed to subwatershed and have important impacts on runoff characteristics. Applying more simplistic hydrologic models to watersheds other than those upon which calibration was conducted is a source of added uncertainty in any application.

A potentially significant source of uncertainty comes from the frequency of water quality sampling, which is difficult to overcome unless substantial resources exist to manually sample at a sub-weekly frequency or operate an extensive network of auto-samplers. Thorough understanding of the dynamics of the local hydrology can aid in strategic sampling based on antecedent moisture, forecasted rainfall, and seasonal factors. This was gained to some degree through this study and should be of value for future sampling efforts.

Additional uncertainty stems from the chosen loading calculation method itself. Study design and nature of the discharge-concentration relationships observed in the data can either increase or limit the appropriate options for methods of load calculation, each with its own set of required assumptions and possible accuracy and precision. A large dataset of concentrations across a broad range of conditions not only improves the input data but better informs the choice of method and may allow for stratification, which has been noted as providing major improvement for most of the available calculation methods (Richards, 1998). Climatological conditions during which a study is conducted clearly have a large impact on the results. The marked difference in hydrologic conditions between these two years is generally seen as a positive for runoff model calibration purposes, however we lack enough data and complexity to accurately represent potentially important components of the hydrologic system that may have important but variable influences under very dry or wet conditions only. This can be particularly true for subsurface dynamics. The differences in hydrology between 2017 and 2018 and that spring runoff was largely not sampled in 2017 mean that comparisons between loading estimates across years are challenging and any resulting differences in nutrient loads may also be due in large part to these factors.

This study provides useful insight into the nutrient transport dynamics of these types of agricultural watersheds in the Lake Champlain Basin. Results serve as a point of reference for not only reducing phosphorus concentrations and loads through implementation of agricultural BMPs moving forward but for study planning and design of monitoring efforts themselves. Researchers and land managers should be prepared to customize their approaches to the hydrogeochemical setting of these waterbodies, aiming to address the sources of uncertainty highlighted herein.

References

- Appling, A. P., M. C. Leon, and W. H. McDowell. (2015). Reducing bias and quantifying uncertainty in watershed flux estimates: the R package loadflex. *Ecosphere*, 6(12), 269. <http://dx.doi.org/10.1890/ES14-00517.1>
- Aulenbach, B. T., and R. P. Hooper. (2006). The composite method: an improved method for stream-water solute load estimation. *Hydrological Processes*, 20(14), 3029–3047. <https://doi.org/10.1002/hyp.6147>
- Aulenbach, B.T., Burns, D.A., Shanley, J.B., Yanai, R.D., Bae, K., Wild, A.D., Yang, Y., and Yi, D. (2016). Approaches to stream solute load estimation for solutes with varying dynamics from five diverse small watersheds. *Ecosphere* 7(6), e01298. <https://doi.org/10.1002/ecs2.1298>
- Cochran, W. (1977). *Sampling Techniques* (3rd ed.) South Orleans, MA. John Wiley & Sons.
- Dalrymple, Tate, and Benson, M.A., (1967), Measurement of peak discharge by the slope-area method: U.S. Geological Survey Techniques of Water-Resources Investigations, book 3, chap. A2, 12 p. Also available at <https://pubs.usgs.gov/twri/twri3-a2/>.
- Harmon, W.R. (1960). *Estimating Potential Evapotranspiration*, (Thesis). Retrieved from <https://dspace.mit.edu/handle/1721.1/79479>. Cambridge, MA: Massachusetts Institute of Technology.
- Limbrunner, J.F., Vogel, R.M., and Chapra, S.C. (2005). A Parsimonious Watershed Model, Chapter 22 in *Watershed Models*, V.P. Singh and D.K. Frevert, Ed., CRC Press, Boca Raton, FL.
- Meals, D., Richards, R.P., and Dressing, S. (2013). *Pollutant load estimation for water quality monitoring projects. Tech Notes 8*, April 2013. Developed for U.S. Environmental Protection Agency by Tetra Tech, Inc., Fairfax, VA, 21 p. Retrieved from <https://www.epa.gov/nps/nonpoint-source-monitoring-technotes>.
- Medalie, L., (2016). Concentration, flux, and trend estimates with uncertainty for nutrients, chloride, and total suspended solids in tributaries of Lake Champlain, 1990–2014: U.S. Geological Survey Open-File Report 2016–1200, 22 p. Available at <https://doi.org/10.3133/ofr20161200>.
- Moriasi, D.N. et al. (2007). Model evaluation guidelines for systematic quantification of accuracy in watershed simulations. *Transactions of the ASABE*. 50(3): 885-900. (doi: 10.13031/2013.23153). Also available at <https://pubag.nal.usda.gov/catalog/9298>.
- National Operational Hydrologic Remote Sensing Center. (2019). *Interactive Snow Information*. <https://www.nohrsc.noaa.gov/interactive/html/map.html>. Accessed 02-11-2019.
- PRISM Climate Group. (2019). *Time-series Values for Individual Locations: 30-yr Climate Normals (1981-2010)*. <http://prism.oregonstate.edu/explorer/>. Accessed 3-16-2019.
- Rantz, S.E. et al. 1982. Measurement and Computation of Streamflow, Volume I: Measurement of Stage and Discharge and Volume II: Computation of Discharge. USGS Water Supply Paper 2175. Available at <http://water.usgs.gov/pubs/wsp/wsp2175/>.
- Richards, R.P. (1998). *Estimation of pollutant loads in rivers and streams: a guidance document for NPS programs*. U.S. EPA Region VIII Grant X998397-01-0, Water Quality Laboratory, Heidelberg University, Tiffin, OH. Retrieved from http://141.139.110.110/sites/default/files/jfuller/images/Load_Est1.pdf.
- Soballe, D. (2017). FLUX32 Help Manual. U.S. Army Corps of Engineers/Minnesota Pollution Control Agency. Available at <https://www.pca.state.mn.us/wplmn/flux32>.

Turnipseed, D.P., and Sauer, V.B. (2010). Discharge measurements at gaging stations: U.S. Geological Survey Techniques and Methods book 3, chap. A8, 87 p. Available at <http://pubs.usgs.gov/tm/tm3-a8/>.

University of Vermont, (2018). High-Resolution Land Cover Mapping of the Lake Champlain Basin. Accessed via <https://www.lcbp.org/publications/high-resolution-land-cover-mapping-of-the-lake-champlain-basin/>. Grand Isle, VT: Lake Champlain Basin Program.

U.S. Department of Agriculture, NRCS. (1986). Urban Hydrology for Small Watersheds. Technical Release 55, 2nd Ed. Available at https://www.nrcs.usda.gov/Internet/FSE_DOCUMENTS/stelprdb1044171.pdf.

U.S. Department of Agriculture, NRCS. (2016). *Helping Farmers Protect Water Quality in the Mckenzie Brook Watershed*. Retrieved from https://www.nrcs.usda.gov/wps/PA_NRCSConsumption/download?cid=nrcseprd1257448&ext=pdf.

U.S. Department of Agriculture, NRCS, (2016). *Vermont Soils Top20 Data Table*. <http://geodata.vermont.gov/#data>. Accessed March 7, 2019.

U.S. Environmental Protection Agency (EPA). (2014) Best Practices for Continuous Monitoring of Temperature and Flow in Wadeable Streams. Global Change Research Program, National Center for Environmental Assessment, Washington, DC; EPA/600/R-13/170F. Available at <https://cfpub.epa.gov/ncea/risk/era/recordisplay.cfm?deid=280013>.

U.S. Naval Observatory. (2019). Sun or Moon Rise/Set Table for One Year. https://aa.usno.navy.mil/data/docs/RS_OneYear.php. Accessed 1-16-2019.

Vaughan, M. (2019). Concentration, load, and trend estimates for nutrients, chloride, and total suspended solids in Lake Champlain Tributaries, 1990–2017: Lake Champlain Basin Program Technical Report No. 86, 77 p. Available at <https://doi.org/10.3133/ofr20161200>.

Vermont Center for Geographic Information. (2016). 0.7 meter Digital Elevation Model - hydro flattened derived from 2013 lidar data (QL2). <http://geodata.vermont.gov/#data>. Accessed March 15, 2019.

Vermont Department of Environmental Conservation. (2017). Vermont Water Quality Standards, Environmental Protection Rule Chapter 29A. Available at <https://dec.vermont.gov/watershed/laws#Existing%20Rules>.